Norwegian University of Life Sciences
Department of Mathematical Sciences and Technology

Master thesis 2014
30 credits

Mobile Agricultural Robot

Independent Four Wheel Ackerman Steering

Jørgen Torgersen

Jørgen Torgersen
Department of Mathematical Sciences and Technology
Norwegian University of Life Sciences
Ås, Norway

This thesis was set in Times Roman by the author, using MiKTEX 2.9.5105 as LATEX implement, TEXmaker 4.1.1 as editor, and Sumatra PDF 2.4 as PDF LATEX output.

Printed and bound in Norway by SiÅs Boksmia.

To my wife, Frida, and my children, Oliver and Isak, who fuels my life with love
To my parents, Lisbet and Jann Eirik, who supports and encourages me
To my sisters, Malin, Siri, and Thea, who inspires me
To my grandfather, Tore, who always stays by my side

Mobile Agricultural Robot

Independent Four Wheel Ackerman Steering

Jørgen Torgersen

Abstract

The main purpose of this master thesis is to develop the kinematic equations for NMBU Mobile Agricultural Robot. A geometrical approach to find the kinematic model is proposed. Kinematic constraints is identified, and a short discussion whether dynamics can be neglected or not is included. As crab steering is wanted on NMBU Mobile Agricultural Robot, a short discussion of the kinematics is presented. Ackerman geometry is introduced, and four wheel Ackerman equations are derived.

Curvature and turning radius is used in the kinematic equations, and a singularity condition is both identified and taken care of. Kinematic equations are developed further for unambiguous steering angles in all wheel positions and separate equations for all four wheels are presented. A map from signed turning radius to inner and outer side is also found, and this gives us unique kinematic equations. Input like signed turning radius and desired speed in center of robot, outputs correct positions and velocity of all actuated joints.

Numerical singularity threshold in singularity workaround are discussed and found. A map from steering angles to number of motor turns is found, as well as a map from ground speed in center of robot to RPM in propulsion motors. An intuitive example where the robot follows a simple path is included. And in the end, two proposals intended to minimize wheel slip when a vehicle is operating in uneven terrain is shown, and the relevance for these system in NMBU Mobile Agricultural Robot is discussed.

A sub-goal is to introduce the concept of mobile agricultural robots, and find a suitable steering system. Battery as energy source is also discussed, and propulsion, traction and frame of NMBU Mobile Agricultural Robot is mentioned. This is one of five thesis's forming a project that aims to design and build a working prototype of a Mobile Agricultural Robot.

Acknowledgements

The author wants to express gratitude to his main supervisor, Dr. Pål Johan From, who took the author and the below mentioned co-students to Brazil for three weeks, learning about mobile robots. The author believes that this project would have been impossible without this "kick off". I also want to thank my main supervisor's wife, Carla for being such a good hostess for us in Brazil. I also want to acknowledge Prof. Nils Bjugstad, my other supervisor, who has enthusiastically guided me through the agricultural part of this thesis, by interesting discussions and literature tips.

This robot project has consisted of the following co-students; Lars Grimstad, his contribution in electronics and motors has been important for this robot. Fredrik Meltzer, his contribution regarding the robots terrain capabilities, and the expected operation time is highly valued. Marit Kristine Svenkerud, her contribution regarding possibilities of implementing Mobile Agricultural Robots in farming is highly regarded. Fredrik Blomberg, his contribution in frame design and productions drawing are very much anticipated.

Thanks to the following people at Federal University of Rio de Janeiro; Dr. Gustavo Medeiros Freitas, for his patient in the flood of questions, and for his professional guidance in the field of motors, gears, encoders and mobile robots. Prof. Fernando Lizarralde, Prof. Liu Hsu, Prof. Ramon R. Costa for sharing their knowledge in robotics to us, and our helpful 3D CAD drawers at UFRJ, Raphael, and Marcel.

The following has also contributed to this thesis; Electro Drives AS, with Ole Egeberg and Rune Einar Westli as key persons, has supplied motors, gears and some electronic for the robot. They have been very helpful, and guided us through selection of components. Dr. Peter Biber from Robert Bosch GmbH (Bonirob Robot), David Dorhout from Prospero Robot, Ann Anderson from Autonomous Tractor Corporation(Spirit), Anders Granmo(friend and farmer at Hattfjelldal Melk DA) and Jann Eirik Torgersen(authors father and farmer at Hattfjelldal Melk DA), Svein Guldal from Bondelaget for ideas, Tore Lervik from Altitech for insight in battery technology, Terje

Thoresen from Røwde tires for good service , Bjørn Brenna from NMBU Mechanical Workshop that built the frame, Tom Ringstad for good advices regarding various electronics, Cong Dung Pham(Ph.D. student in robotics at NMBU) for ideas and discussions, Prof. Bjørn Fredrik Nielsen for mathematical guidance and thesis writing tips, Kim and Ingvild Storvold for last minute correction.

Although not directly related to this thesis, the author wants to express his thanks to following persons at Stabburet A/S Avd Sunda: Ståle Snartland, Finn Bjerknes, Thomas Torkildsrud, Christopher Farstad Hulme og Terje Falldalen, for giving him the opportunity to learn about machines, peoples and work life.

During this master thesis the author has received support from NJF (Nordic Association of Agricultural Scientist, CAPES-SIU-2013/10076 and Matsatsingen at NMBU(Norwegian University of Life Sciences).

J.T.

Contents

Glossary, Notation and Acronyms **xv**

List of Figures **xxiii**

List of Tables **xxvii**

1 Introduction **1**
1.1 Robot 1
1.1.1 Mobile Robots 2
1.2 Robots in farming today 2
1.3 Robots in farming tomorrow 3
1.3.1 Precision Farming 3

2 Concept **5**
2.1 Farming done today 6
2.1.1 Soil compaction 7
2.1.2 Person hours 9
2.2 Artificial intelligence needed for Mobile Agricultural Robots . 9
2.3 Challenges for Mobile Agricultural Robots 10
2.3.1 Human safety 11
2.4 Comparison of robots similar to NMBU Mobile Robot 11
2.5 Other Concepts 14
2.5.1 Autonomous Tractor Corporation 14
2.5.2 Prospero 15
2.6 NMBU Mobile Agricultural Robot 16
2.6.1 Brazil 16
2.6.2 Rethink Farming 17
2.6.3 Requirements 17
2.6.4 Early Specification 17

I Electromechanical design **19**

3 Steering System **23**
3.1 Differential Drive Steering 23
3.2 Frame Articulated Steering 24
3.3 Four Wheel Steering 25
3.4 Steering Evaluation 26
3.5 Steering Components 28
3.5.1 Electric Servomotors 28
3.5.2 Reduction Gears 29
3.6 Encoders and Absolute Position 31
3.6.1 Incremental Encoder 32
3.6.2 Absolute Encoders 33
3.6.3 Practical Implementation 34

4 Energy source for NMBU Mobile Robot **35**
4.1 Specific Energy 35
4.2 Lithium Batteries 36
4.2.1 State of the art 36
4.2.2 $LiFePO_4$ Technology 37
4.3 Battery for NMBU Mobile Robot 37
4.4 Faulty wiring from supplier created short circuit 38
4.4.1 Actual voltage of 48 Volt $LiFePO_4$ battery pack 39
4.4.2 Battery formulas 39
4.5 Battery change 42
4.6 Battery Managements Systems 42
4.7 Emergency Stop System on NMBU mobil robot 42

5 Propulsion **43**
5.1 Propulsion Components 43
5.1.1 Propulsion Motor 43
5.1.2 Reduction Gear 44
5.1.3 Motor controller 44
5.1.4 Practical Implementation 45
5.1.5 Encoder 46

6 Traction and Frame **49**
6.1 Tracks versus wheels 49
6.1.1 Tracked vehicles 49
6.1.2 Advantages of tracks 51
6.1.3 Benefits of wheels 51

6.1.4 Wheels on NMBU mobile robot . . . 52
6.2 Frame . . . 55

II Independent Four Wheel Ackerman Steering 59

7 Kinematic Model 63
7.1 Inverse Kinematics . . . 64
7.1.1 Kinematic Constraints . . . 64
7.1.2 Dynamics . . . 64
7.2 Crab Steering . . . 65
7.3 Ackerman Geometry . . . 66
7.3.1 Four Wheel Ackerman Equations . . . 67
7.4 Curvature and Turning Radius . . . 69
7.4.1 Singularity Workaround . . . 71
7.5 Kinematic Equations . . . 71
7.5.1 Unique steering angles . . . 72
7.5.2 Individual angle equations . . . 73
7.5.3 Mapping signed turning radius to local end-effectors . . . 74
7.6 Practical Implementation of Steering . . . 75
7.6.1 Numerical Singularity Threshold . . . 76
7.6.2 Propulsion Motor Kinematics . . . 77
7.6.3 Servo Motors Positions . . . 78
7.6.4 Example . . . 79
7.7 Advantages . . . 82

8 Minimizing wheel slip in uneven terrain 83
8.1 Measure Vertical Acceleration Proposal . . . 83
8.2 Constant Torque Proposal . . . 85
8.3 Relevance for Mobile Agricultural Robots . . . 85

9 Conclusion 87
9.1 Part II . . . 87
9.2 Introduction and Concept . . . 87
9.3 Part I . . . 88

Bibliography 91

Glossary, Notation and Acronyms

$[\dot{x}, \dot{y}, \dot{\theta}]^T$	Vector representation of motion in the plane
$\dot{\theta}$	angular speed
$\dot{x}$	speed in x-direction
$\dot{y}$	speed in y-direction
∞_t	singularity test
κ	curvature
ω	angular speed
τ_{pn}	Nominal propulsion torque
τ_{pp}	Peak propulsion torque
θ_i	angle for the inner wheel
θ_o	angle for the outer wheel
θ_{fi}	angle front inner wheel
θ_{fo}	angle front outer wheel
θ_{lf}	angle left front wheel
θ_{lr}	angle left rear wheel
θ_{rf}	angle right front wheel
θ_{ri}	angle rear inner wheel

θ_{ro}	angle rear outer wheel
θ_{rr}	angle right rear wheel
A_s	Surface area of tracks or tires
Bt_h	Burn time of battery in hours
C_s	sign changer
D_{ci}	Irretrievable compaction damage
F_s	Load of the machine
Nt	number of turns that the servo motor need to travel to
Nt_{lf}	number of turns that the left front servo motor need to travel to
Nt_{lr}	number of turns that the left rear servo motor need to travel to
Nt_{rf}	number of turns that the right front servo motor need to travel to
Nt_{rr}	number of turns that the right rear servo motor need to travel to
P_s	Surface pressure
r	radius
R_t	turning radius
R_t and S	Turning radius and center of robot speed is geometrical representation of motion in the plane
RPM	rounds per minute
RPM_{ls}	RPM left side propulsion motor
RPM_{rs}	RPM right Side propulsion motor
S_i	speed inner wheel

S_o	speed outer wheel
S_{lr}	wheel speed right side
S_{ls}	wheel speed left side
T_w	Half track width
v_h	The needed speed increase for the wheel meeting the local heightening
v_x	speed in x-direction
v_z	speed in z-direction
$v_z(t_{i+1})$	measured speed in z-direction
W_b	Half wheel base length
4WD	Four Wheel Drive
4WS	Four Wheel Steering
Ackerman	Geometric solution to calculate the different steering angle of the inner and outer wheel due to that the inner and outer wheel tracing out circles of different radius.
Acre	The acre is a unit of area used in the imperial and U.S. customary systems. It is equivalent to 43,560 square feet. An acre is about 40 percent of a hectare – slightly smaller than an American football field
Ah	Ampere hours
AMS	Automatic Milking Systems
APS	Area Positioning System
ATC	Autonomous Tractor Corporation
ATV	All-Terrain Vehicle
av	Average

BLDC	Brush-less DC
BMS	Battery Management System
CAD	Computer-aided design (CAD) is the use of computer systems to assist in the creation, modification, analysis, or optimization of a design.
CAN bus	Controller Area Network is a vehicle bus standard designed to allow microcontrollers and devices to communicate with each other within a vehicle without a host computer
CANopen	CANopen is the internationally standardized (EN 50325-4) CAN-based higher-layer protocol for embedded control system.
Crop	Volunteered or cultivated plant whose product is harvested by a human at some point of its growth stage
diesel-electric	A diesel-electric transmission system includes a diesel engine connected to an electrical generator, creating electricity that powers electric traction motors.
Energy density	$\frac{KWh}{l}$
Fertilizing	Adding organic or non-organic material to the soil to supply one or more plant nutrients essential to the growth of plants
Field	Arable land
Gallon	3.78541178 litre
GPS	Global Positioning System
h	Hour

Haptic	Tactile feedback technology which recreates the sense of touch by applying forces, vibrations, or motions to the user
Harrowing	Is an implement for breaking up and smoothing out the surface of the soil
Headland	Area at each end of a planted field, also called turn-row. It is used for turning around with farm implements during field operations.
Holonomic	A robot is holonomic if the controllable degrees of freedom are equal to the total degrees of freedom, and it can move instantly in any direction
hp	horsepower
ICR	instantaneous center of rotation
Implement	Agricultural machinery used in the operation of an agricultural area or farm.
IMU	inertial measurement unit
Inverse Kinematics	Use of the kinematics equations of a robot to determine the joint parameters that provide a desired position of the end-effector
kJ	Kilojoule
kph	Kilometre per hour
kWh	Kilowatt hour
l	litre
$LiFePO_4$	Lithium Iron Phosphate
N	Normal force
n/a	Not applicable
NIA	No information available

NMAR	NMBU Mobile Agricultural Robot
NMBU	Norwegian University of Life Sciences
Organic fertilizer	Feces from animals on the farm, also called manure, there are two types, dry or slurry
Path	A slope that the robot should follow
Pesticides	Substances meant for attracting, seducing, destroying or mitigating any pest, also known as plant protection
Phytotechnology	Plant Level Husbandry
PID	A proportional-integral-derivative controller is a control loop feedback mechanism widely used in industrial control systems
ROS	The Robot Operating System (ROS) is a flexible framework for writing robot software. It is a collection of tools, libraries, and conventions that aim to simplify the task of creating complex and robust robot behaviour across a wide variety of robotic platforms.
RTK	Real Time Kinematic
Singularity	A point at which a given mathematical object is not defined or not well-behaved, for example infinite or not differentiable
Skid steering	Turning by generating differential velocity at the opposite sides of the vehicle
Slodden	A tool used to even out the soil after ploughing
SOC	State Of Charge

SOH	State Of Health
Sowing	To scatter seeds over the ground for growing
Specific energy	$\frac{KWh}{kg}$
Tool	Removable application inside the frame of the robot made for a specific task. Sowing machine is a example of a tool
UFRJ	Federal University of Rio de Janeiro
V	Volt
v	Velocity
Weeding	Removal of plants considered undesirable, unattractive, or troublesome, especially one growing where it is not wanted
wrt	with respect to

List of Figures

1.1 Other areas that are automated in farming today are feeding, cleaning and cow brushing. 2
1.2 A brief presentation of the ideas in future farming by Harper Adams University, England, courtesy of Blackmore [2012]. . . 3

2.1 Shows why we need more precision in agriculture today, here a productive land is wasted to a significant extent and a robot using GPS-RTK system would improve seeding coverage. Picture taken by the author 11 May, 2014 in Ås, Akershus. 6
2.2 Shows a wet area that a conventional tractor got stuck in, it is also easy to see the unproductive area that this created. A light weight tracked robot could avoid this. Picture taken by the author 11 May, 2014 in Frogn, Akershus. 6
2.3 Soil compaction depends one several factors, the most significant are shown here. 7
2.4 Wet harvesting may cause soil compaction, courtesy University of Kentucky. 8
2.5 The robots compared in table 2.3 on page 12 are shown above 13
2.6 The Spirit with Terry Anderson (of Norwegian ancestry), see section 2.5 on page 14 for more information, courtesy of Autonomous Tractor Corporation [2013]. 14
2.7 A Prospero analysing the soil before a suitable seed is planted [Dorhout, 2013]. 16

3.1 Pioneer *P3-AT MOBILE ROBOTS* skid steered mobile platform with 7 degrees of freedom manipulator used for haptic control algorithm research at NMBU. 24
3.2 Articulated steered modern Case IH STX 530 Quadtrac at the Maldon Working day 2011, courtesy tractors.wikia.com. 25
3.3 Four wheel steered Seekur is a all-weather, outdoor robot platform for outdoor research, courtesy Adept MobileRobots . . . 26

3.4 Shows the different steering schemes evaluated for the NMBU mobile robot in a right turn. 27
3.5 An exploded view of the steering components [Blomberg, 2014]. 28
3.6 Some of the mechanical components used in the steering system. 30
3.7 Some of the control components used in the steering system. . 32

4.1 Energy components. 38
4.2 Faulty wiring on the battery created a short circuit when connecting battery to the charger 41

5.1 An exploded view of the propulsion components.[Blomberg, 2014] 44
5.2 The main components of the propulsion system 45
5.3 This figure shows the table we used to identify which one of the six possible hall sensors connections that were correct. The top row is the Roboteq's Norwegian color codes, the six row beneath are the color codes for the motor side and together they cover the six possible wirings. Number four from the bottom and the top one is the only one that worked in open loop, and since the top one is the only connection that was possible to run in closed loop mode, this is identified as correct. 47

6.1 Normally when ploughing, either the left or right wheel pair tracks the exposed furrow, and this amplifies soil compaction. The tractor shown above has both wheel pairs on the unploughed land, and this reduces soil compaction to some extent [Bjugstad, 2014]. A Caterpillar Challenger MT765B tracked tractor at work ploughing a field near to Leverton Lucasgate, Lincolnshire, Great Britain. The photo was taken on 22 October 2008.[Billinger, 2008]. 50
6.2 shows the five tires auditioned at Røwde AS for NMBU Mobile robot. Photo taken by the author. 53
6.3 Fredrik Meltzer to the left and Lars Grimstad to the right in the background when the chosen tire is mounted on the rim by Terje Thoresen. Photo taken by the author. 54
6.4 This figure shows a rendering from SolidWorks of the frame shoving the tool replica as the triangle in the middle of the robot [Blomberg, 2014]. 56

7.1 This figure shows how crab steering mode follows a path . . . 66

7.2 In this figure the four wheel Ackerman geometry is shown while the robot is making a left turn. It is from this figure that the equations presented in this chapter is derived from. . 67
7.3 This figure shows a randomly chosen path that the Robot should follow. 70
7.4 This figure shows each wheels individual steering angle in ° given from the same reference axis shown in the top middle of the figure. Note when driving straight forward all wheels are at 180°. 72
7.5 This figure shows how the singularity threshold can be found, given a constraint in precision of 4 cm. 76

8.1 This figure shows the two different paths that wheels need to follow, and it is shown that the upper wheel in this figure needs to go faster during the event of the local heightening if the two wheels should be at the same x-coordinate at the same time. . 84

List of Tables

2.1 This table shows the various farm operations parameter on a typical Norwegian farm. Note*May differ between farms. Note**Tool dependant. Note***Only applicable on farms with animals 10
2.2 This table shows the challenges different robots has to cope with, and notice that the agricultural robots are facing the largest confrontations. [Edan et al., 2011] 11
2.3 Comparison of agricultural robots. 12
2.4 Requirements of NMBU Mobile Robot. 18
2.5 Early specifications of the NMBU Mobile Robot. 18

3.1 A table similar like the one used in [Shamah et al., 2001] is used for steering system evaluation. This table lists the most important topics for our robot at the top, and then gradually presenting less important features further down. 27

4.1 This table gives a comparison of different Lithium Ion Cathodes used With carbon Anodes [Lawson, 2014]. 36

7.1 This table show the kinematic constraint in the NMBU mobil robot, see section 7.6.2 on page 77 and section 7.5 on page 71 for more details 64

Chapter 1

Introduction

The main purpose of this master thesis is to develop the kinematic equations for NMBU Mobile Agricultural Robot. A contribution using a geometrical approach to find the kinematic model is proposed. Kinematic constraints is identified, and a short discussion whether dynamics can be neglected or not is included. As crab steering is wanted on NMBU Mobile Agricultural Robot, a short discussion of the kinematics is presented. Ackerman geometry is introduced, and four wheel Ackerman equations are derived.

A sub-goal is to introduce the concept of mobile agricultural robots, and find a suitable steering system. Battery as energy source is also discussed, and propulsion, traction and frame of NMBU Mobile Agricultural Robot is mentioned. This is one of five thesis's forming a project that aims to design and build a working prototype of a Mobile Agricultural Robot.

1.1 Robot

> "A robot is a versatile mechanical device - for example, a manipulator arm, a multi joint multi fingered hand, a wheeled or legged vehicle, a free flying platform, or a combination of these - equipped with actuators and sensors under the control of a computing system. It operates in a workspace within the real world. This workspace is populated by physical objects and is subject to the laws of nature. The robot performs task by executing motions in the workspace."[Latombe, 1991]

1.1.1 Mobile Robots

Characterisation of mobile robots are done by their ability to move around freely in their environment, and they differ from conventional industrial robots by their possibility to locomote in a given environment, and also possibly between different environments [From et al., 2014]. The human invented actively powered wheel is perhaps the the most efficient way to achieve locomotion on flat ground [Siegwart et al., 2011], and it can be fitted with tracks, to reshape the wheel into a form that achieves good locomotion capabilities in non-flat soft surfaces.

1.2 Robots in farming today

Robots have traditionally been used for tasks that are categorized as; Dull, Dirty, and Dangerous, also known as the three D's in robotics. Although this phrase is old, it describes the semi-manual milking process of cows well[1]. Automatic Milking Systems (AMS) were first introduced on a commercial farm in 1992 and it is intended to make the physical assistance of the farmer during milking of each cow unnecessary. The first systems only replaced the milking parlour, but today they milk 35% [Nodeland, 2013]of all Norwegian cows, and integrates management functions like milking frequency, individual feeding, cow traffic, monitoring milk quality, and cow fertility [Meskens et al., 2001].

(a) DeLaval swinging cow brush SCB, courtesy DeLaval.

(b) Lely Discovery 90SW barn cleaner, courtesy Lely.

(c) The Combi Feeder Robot from Ing. Bräuer GmbH Stalltechnik.

Figure 1.1: Other areas that are automated in farming today are feeding, cleaning and cow brushing.

[1]The author has grown up on a dairy farm and can confirm this

(a) Vision of new generation of robots poised to transform global agricultural production, here seen crop scout seeding, courtesy of Blackmore [2012].

(b) Vision of new generation of robots poised to transform global agricultural production, here seen crop scout harvesting, courtesy of Blackmore [2012].

Figure 1.2: A brief presentation of the ideas in future farming by Harper Adams University, England, courtesy of Blackmore [2012].

1.3 Robots in farming tomorrow

Robots in farming today work in a more or less known environment, and the next phase is to get the robots out of the barn and into the fields. Since there already has been done significant research in mobile robots, we mainly need to focus on farm-technical issues. In the same process one should rethink how farming is done today, and put the plants need first. Development of small intelligent agricultural robots allows us to do this, as they can perform operations not possible today, that either were found to expensive or time consuming. Social impact of this paradigm is improved public perception of agriculture, as small vehicles makes public acceptance and liability easier [Blackmore, 2012]

1.3.1 Precision Farming

Traditional farming supports one rate of additive or manipulation per field, where precision farming can have a variable rate of additive or manipulation within a field supporting local variations, and the optimum solution for some crops may be single plant care, see figure 3.5 on page 28, also called plant level husbandry (phytotechnology) [Blackmore, 2012]. This high definition farming gives higher yield per square meter, with greatly reduced herbicide and pesticide use and with the possibility to decrease water and fertilizer usage[Blackmore, 2012].

Chapter 2

Concept

A sub-purpose of this master thesis is to introduce the concept of Mobile Agricultural Robots. There are many drawbacks in today's way of farming. Soil compaction is one of the most important problems that has to be addressed, and is the result of heavy machinery on the fields. Tillage equipment then has to dig deep in order to aerate the soil, and to reach far enough down a big tractor is needed, and we find our self in a vicious circle. Bennedsen [2009] claims that 90% of today's total diesel usage in agricultural operations goes to repair the damages from soil compaction. Increased precipitation caused by climate changes, will also make it difficult for today's farming machinery to operate in the future.

This problem can be minimized by reducing the weight of the farming equipment significantly, and to keep the coverage per time as before, more units will need to be deployed. In countries where wages are low, this units could be operated by workers, whereas in high cost areas around the world this will not be possible. Hence the solution proposed here is to make the farm equipment autonomous, such that the farmer still can cover the same area per time with possibly lower cost.

Energy expenditure is unnecessary large with heavy equipment. Usually the tractor and tool forms a long trailer with a large turning radius, and when the tractor trailer has come to the end of the field, it must use headland in order to change direction. This headland has to be completed at a later stage and increases both time and fuel usage. Small omnidirectional robots with the tool inside the frame completely eliminate the headland, and improve fuel economy. For a more in-depth coverage the concept and the future of robotic farming see Svenkerud [2014].

2.1 Farming done today

Today farming is done with big tractors driven by an operator, in most cases the farmer himself. The reason for using a big tractor is that it is possible to mount big tools that either has the capability of completing several steps like harrowing, sowing and compacting, or that the tools has significantly increased working width. Those implements mean faster coverage and this frees up time in the critical time window a farmer might face e.g. between heavy rain falls.

Figure 2.1: Shows why we need more precision in agriculture today, here a productive land is wasted to a significant extent and a robot using GPS-RTK system would improve seeding coverage. Picture taken by the author 11 May, 2014 in Ås, Akershus.

Figure 2.2: Shows a wet area that a conventional tractor got stuck in, it is also easy to see the unproductive area that this created. A light weight tracked robot could avoid this. Picture taken by the author 11 May, 2014 in Frogn, Akershus.

2.1.1 Soil compaction

Soil compaction is a detrimental phenomena occurring both in the surface of the soil and deeper down in the profile, and whereas the surface compaction is alleviated by tillage operations, the damages further down may be irreparable [Bjugstad, 2014].

By volume, typical soil consists of 25 percent water, 25 percent air, and 50 percent organic matter and soil particles, when soil is at field moisture capacity. Soil compaction occurs when the force of the wheel traffic forces the aggregates together. If the applied force is great enough, the aggregates is destroyed. As a result, the soil gets dense with few large pores, and this gives poor internal drainage and reduced aeration, seeNolte and Fausey [2013] and Frisby and Pfost [1993] for more information.

A disadvantage by using big farming equipment is that their heavy weight creates soil compaction, see figure 2.4 on the next page for illustration. The problem occurs when the wheels of the machine are in contact with the soil, and the problem gets worse when the soil is wet[Wolkowski and Lowery, 2008], as seen in figure 2.3b.

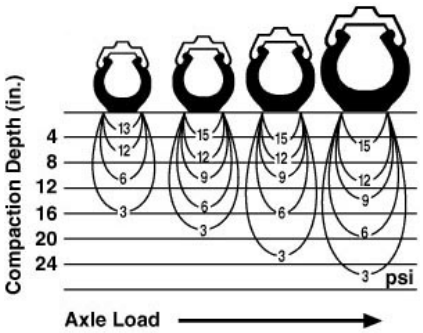

(a) Here it is shown that soil compaction increases while axle load is increased [DeJong-Hughes et al., 2001].

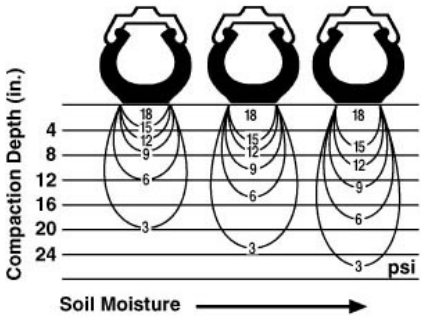

(b) Here it is shown that soil compaction is increased when soil is wet [DeJong-Hughes et al., 2001].

Figure 2.3: Soil compaction depends one several factors, the most significant are shown here.

Most farmers are aware of this problem, but the significance is often underestimated. The effect of soil compaction on crop yield may be an important factor in today's farming economy, and there are findings that suggest soil compaction can reduce crop yields up to fifty percent, see Wolkowski and Lowery [2008].

One might think that it is easy to compensate for this problem by adding

Figure 2.4: Wet harvesting may cause soil compaction, courtesy University of Kentucky.

wider tires, or tracks to distribute the load of the machine F_s on a wider surface area A_s. This is a misconception, see figure 2.3 on the previous page. Although the surface pressure P_s is reduced by this approach, as seen below:

$$P_s = \frac{F_s}{A_s} \tag{2.1}$$

Irretrievable compaction damage D_{ci} further down the soil profile is not addressed, as this factor only depends on the load of the machine, see Bjugstad [2014], as seen below:

$$D_c = F_s \tag{2.2}$$

Compensation for the increased load will not be realized, and this approach only spreads the surface compaction problem over a wider area, see [Wolkowski and Lowery, 2008]. The only way to reduce soil compaction is to

1. Avoid operations when the soil is wet[1]
2. Decrease vehicle loads, i.e lighter machines
3. Manage vehicle traffic on the field so minimum soil compaction can be realized[2]. This easily accomplished with GPS-guide steering

2.1.2 Person hours

A problem farmer's face today is long working hours during the spring work, harvesting period and preparation for next year. They spend hours sitting on tractor and doing operations that a robot could do.

Farmers in countries that have high wages might not have the economy to hire an operator to drive the tractor, instead they have to do this time consuming task on their own. They usually have other things to take care of as well like maintenance of the farm, milking cows and feeding the animals. If all this comes in addition to a family life where the wife work full time, which in most cases are necessary , the farmers have to work both the day shift and the night shift during certain periods. This makes the profession less desirable for young people, and a farmer's hourly wage can become low.

2.2 Artificial intelligence needed for Mobile Agricultural Robots

One solution for the farmers is to deploy robots to the field for low level tasks. Operations that a robot easily can do is ploughing, slodden , harrowing, and weeding. The main challenges here is that one need powerful robots that has a lot of energy stored. Hence these robots could be diesel-electric system, like figure 2.6 on page 14.

Examples of operations that requires a bit more intelligence is sowing, fertilizing, and spraying pesticide. The reason for this step up in intelligence is that the robot need to sense when to fill up, how to fill up and where to begin again. The demands for precision are also higher in this group. A

[1]This is not always a option, the crop might be ready for either planting or harvesting and their time frame short. Farmers want to have equipment that can cope with such challenges, and mobile light weight tracked robots might be a solution

[2]There are common understanding that the most soil compacting happens the first time the wheel travels a path see [Wolkowski and Lowery, 2008], it therefore advised to use the same wheel paths every time driving in the same field

Farm operation	**Time spent per session**	**Frequency***	**Power requirement Robot**	**Artificial intelligence needed****
Ploughing	High	Low	High[Stout and Cheze, 1999]	Low
Slodden	Medium	Low	High	Low
Organic fertilizer***	Low	Medium	High	Medium
Harrowing	Medium	Low	High[Stout and Cheze, 1999]	Low
Sowing	High	Low	Low	Medium
Compacting	Medium	Low	Medium	Low
Artificial fertilizer	Low	High	Low	Medium
Spraying pesticides	Low	Low	Low	Medium/High
Harvesting	High	High	High	High
Weeding	High	High	Low	Medium/High

Table 2.1: This table shows the various farm operations parameter on a typical Norwegian farm. Note*May differ between farms. Note**Tool dependant. Note***Only applicable on farms with animals

reason for this is that the product put in the soil is expensive, and deploying to much or to little product harms the crop.

Operations that require the highest intelligence are probably harvesting of high value crop. The machinery used in this process is advanced, and they often require a skilled operator. Some crops are still manually harvested because of their complexity, these tasks demand an intelligent mobile robot with possibly several manipulators.

2.3 Challenges for Mobile Agricultural Robots

The list of challenges in mobile agricultural robotics is long, and this section briefly covers the main challenges. A mobile agricultural robots need to operate in a open area, where the environment and target are partly unknown, see From et al. [2014] and Edan et al. [2011], and this demands robots with

higher cognitive abilities. Even though the physical appearance of a field is fixed with respect to a frame, configuration of the field may vary from year to year, and the tools needed to do various task, changes trough out the season.

	Industrial robots	**Space, Underwater, and Military robots**	**Medical robots**	**Mobile agricultural robots**
Environment	Known	Unknown	Known	Unknown
Target	Known	Known	Unknown	Unknown

Table 2.2: This table shows the challenges different robots has to cope with, and notice that the agricultural robots are facing the largest confrontations. [Edan et al., 2011]

2.3.1 Human safety

Human safety becomes a significant concern when we move the robots out from their controlled environment. Smaller robots greatly reduce this concern, see for example Blackmore [2012]. For research purposes this is less relevant, as the robot can be operated in controlled manners.

2.4 Comparison of robots similar to NMBU Mobile Robot

In the beginning of this project a comparison between other robot design were conducted. There have been build quite a few mobile agricultural robots in the past, but unfortunately, the available documentation on internet is wage. This is easily seen in table 2.3 on the next page, and the many NIA(No Information Available). One reason for this is that the designers want to protect their ideas and design, and that is understandable. The search were narrowed down to robots that are similar in size and configuration as NMBU mobile robot. The reason for this comparison was to verify our robots frame, propulsion system, steering system, battery system and technical design. This comparison is presented in table 2.3 on the following page.

	Mobile Robot for Weeding. [Madsen and Jakobsen, 2001]	**BoniRob. [Biber, 2014]**	**Mobile Agricultural Robot. [Tabile et al., 2011]**	**Kongskilde Robotti. [Green, 2013]**
Country and year	Denmark 2001	Germany 2014	Brazil 2011	Denmark 2013
Application	Weeding	Tool dependent	Data collection	Weeding
Project type	Research	Commercial	Research	Commercial
Speed	6.3 kph	13 kph	NIA	5 kph
Burn time batteries	2-4 h	6 h	24 h	NIA
Weight	312 kg	(800-1000) kg	NIA	<500 kg
Length and width, cm	100 x 100	150 x 150	200 x (120-200)	NIA
Ground clearance	50 cm	80 cm	NIA	NIA
Frame material	Aluminium	Steel	Steel	NIA
Drive-train	4WD	4WD	4WD	Tracks
Propulsion motors	4 x 150 W	Couple of 100 W	4 x 750 W	2 x 5000 W
Propulsion gearing	1:9.3	NIA	1:75	NIA
Steering system	4WS Ackerman	4WS Ackerman	2WS Ackerman	Skid steering
Steering motors	NIA	Couple of 100 W	4 x 150 W	n/a
Steering gearing	NIA	NIA	1:230	n/a
Suspension	Passive	Passive	Passive	Passive
Battery technology	Gel	Lead	NIA	Lead
Battery weight	60 kg	NIA	NIA	NIA
Battery energy	1.68 kWh	NIA	7.8 kWh	5.28 kWh

Table 2.3: Comparison of agricultural robots.

(a) BoniRob is a multi directional mobile robot that uses the app-concept by allowing different tools to be added or removed as needed. The track width of BoniRob is adjustable [Biber, 2014].

(b) Robotti is a electric tracked autonomous agricultural robot that uses various demountable implements, intended for plant production [Green, 2013].

(c) Agricultural Mobile Robot is intended for for long operation time while collecting agricultural field data [Tabile et al., 2011].

(d) Mobile Robot for weeding is one of the first attempts on designing a autonomous mobile agricultural robot [Madsen and Jakobsen, 2001].

Figure 2.5: The robots compared in table 2.3 on the facing page are shown above

2.5 Other Concepts

There have been built quite many mobile agricultural robots in the past. They differ in size, some are rather large like figure 2.6, others are tiny legged robots designed to operate in swarms, see figure 3.5 on page 28.

2.5.1 Autonomous Tractor Corporation

Figure 2.6: The Spirit with Terry Anderson (of Norwegian ancestry), see section 2.5 for more information, courtesy of Autonomous Tractor Corporation [2013].

Spirit is a mobile robot that has 300 hp on-board. The first versions was a driver-less tractor with tools or implements mounted traditionally behind or in the front of the robot, and large tools required mounting on a trailer behind the robot. Recently their focus has changed towards driver-less implements[3].

[3]This the same thing that happened to us, we first decided to have the tool behind the NMBU robot, but we ended up with the tool inside the frame

They believe that it is more efficient to carry the tool, than pushing or pulling it.

It is a diesel-electric system with a 400 gallon diesel tank. This gives the Spirit 36 hours of autonomous operation. Up to 16 modules can be working together for fast coverage[4].

One interesting thing is that Spirit don't use GPS for positioning, ATC uses a system they call Area Positioning System (APS) and it uses the combination of computers, lasers and radio transmissions to perform these tasks. Four transponders are placed around the field, and two transponders are placed one the robot. The six transponders all have status as masters, and they communicates to each other. ACT says that the system is more accurate than GPS. There have been reported problems with down time regarding GPS in farming in other publications, see Oksanen [2013].

2.5.2 Prospero

Prospero is a working prototype of small robots that uses a combination of swarm and game theory to operate as an Autonomous Micro Planter, see [Dorhout, 2013]. The current version is the first of four phases. They are meant to be used as a group or a swarm. The remaining three steps are a robot that can tend the crop, a robot that can harvest the crop, and the last step is a robot that can plant, tend, and harvest the crop autonomously.

The main advantage of this type of robot is that it has the ability to farm inch by inch, meaning that it can analyse the soil before planting each seed, and thus planting the most appropriate seed for that spot. This contributes to a higher productivity of that acre.

[4]This is meant to be implemented for the NMBU robot as well,section 2.6.3 on page 17

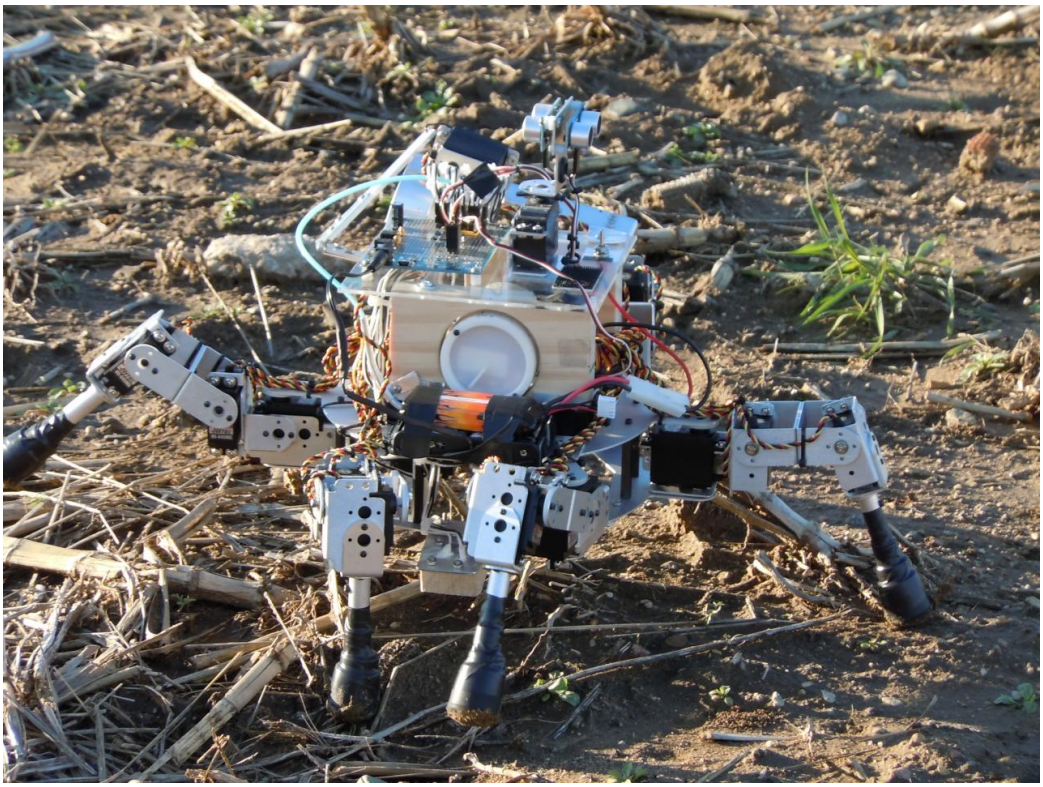

Figure 2.7: A Prospero analysing the soil before a suitable seed is planted [Dorhout, 2013].

2.6 NMBU Mobile Agricultural Robot

This master project proposal were first presented by my main supervisor Pål Johan From, spring 2013, under a master thesis project meeting. He presented Mobile Agricultural Robot as one possible master thesis project, and five master students, including the author chose this project. A trip to Denmark learning about agricultural robots were completed summer 2013, and in the autumn the meeting frequency increased. In November 2013 the concept; Lightweight Modular Mobile Agricultural Robots, where presented by Pål and my second supervisor Nils Bjugstad as main focus the master project.

2.6.1 Brazil

In January 2014 the project participants went to Rio De Janeiro, Brazil, to learn more about mobile robots, motors, and encoders. During our stay in Brazil, a comprehensive literature search were done, and we gradually started

the process of deciding how our mobile agricultural robot should look like, how large it should be, how it should steer, where the tool should be and so forth. A rectangular shape of the robot where the first thing that where decided, and since tool-working-width defines efficiency, the robot became significantly wider, than long.

2.6.2 Rethink Farming

In trend with Blackmore [2012], we quickly dismissed our first traditional proposal of pulling the tool after the robot. Instead the different tool modules is going to placed inside the frame of the robot. This gives better mobility, as equal normal forces is obtainable on each wheel since the center of mass is located in the center of robot. The steering configuration were also discussed, and independent four wheel steering were chosen for it's flexibility. This makes the NMBU mobile robot capable of zero turning radius, two and four wheel Ackerman, differential drive or skid steering, and crab steering.

2.6.3 Requirements

The first task that needs to be done when building robots is the development of requirements, as they point directions for design, software architecture, calculations and component choices. As this is a important part of robot building, and the author and his co-students had little experience in robots, the basic requirement where presented by Pål before Christmas 2013. Later on this requirements were refined January 2014 during the stay in Brazil, and the result is shown in table 2.4 on the following page.

2.6.4 Early Specification

After the requirements were set in section 2.6.3, decisions regarding size, weight and operating speed were made. During this part, farmers were contacted to identify necessary payload for a given coverage of artificial fertilizer, the physical shape of different tools were examined, how fast or slow a tractor need to operated and so fourth. Different types of terrain that the robot should operate in were also examined and the result of this this small study is presented in table 2.5 on the following page.

Mobile	For coverage of large fields
Small turning radius	Minimize headland area and increase manoeuvrability
Light weight	Minimize soil compaction
Good locomotion capabilities	Cope well with different environments
Battery-driven	Ease of control and environmentally friendly
Tool independent	One robot for multiple tasks minimizes the the down time and makes investment economically sustainable
Scalable	Several robots should be able to work as a team for fast coverage of fields
Cheap	So a team of robots is possible to own or rent by a farmer

Table 2.4: Requirements of NMBU Mobile Robot.

Total mass fully loaded	300 kg
Payload	100 kg
Tool weight	50 kg
Wheel diameter	400 mm
Operating velocity	5 kph
Length and width	1100 mm x 1700 mm
Minimum ground clearance	300 mm

Table 2.5: Early specifications of the NMBU Mobile Robot.

Part I

Electromechanical design

Summary part I

A sub-purpose of this master thesis is to find a suitable steering system for NMBU Mobile Agricultural Robot. This master thesis also covers batteries as energy source for NMBU Mobile Agricultural Robot. In addition this master thesis covers the propulsion and traction system of NMBU Mobile Agricultural Robot and mentions the main ideas for frame design on NMBU Mobile Agricultural Robot. This part covers everything mentioned above, except the concept.

Different steering schemes suitable for NMBU Mobile Agricultural Robot are evaluated, and four wheel steering is chosen. Steering components consisting of brush less servo motor and reduction gear is present and we discuss the practical implementation those. Encoders needed for joint position is then introduced, and we discuss various ways to achieve absolute position.

The preferred energy source for NMBU Mobile Agricultural Robot is presented, and we compare the specific energy in diesel and batteries. Lithium batteries is introduced and both state of the art, and chosen battery discussed. Useful battery formulas are presented, and we discuss how to change battery autonomous during operation. Importance battery managements systems are further discussed, and emergency stop system on NMBU Mobile Agricultural Robot is explained.

Propulsion components consisting of brush less motor and reduction gear are introduced, and practical implementation wrt hall sensors and encoders is discussed. A discussion whether we should implement tracks or wheels is carried out, and various tires for NMBU Mobile Agricultural Robot is presented and evaluated. The main idea behind the frame design is present, and we explain the advantages of this solution.

Chapter 3

Steering System

3.1 Differential Drive Steering

A criterion given by the concept; Agricultural Mobile Robots, is that the robot should have high manoeuvrability, and this section only covers steering schemes that meet this requirement, see table 2.4 on page 18.

Skid steered vehicles, also called differential driven vehicles, turn when the wheels or track on one side, operates at a different speed than the opposite side. The two sides must therefore be driven independently, and the wheels or track on the same side is normally mechanically locked and synchronized to each other. The system turns in the direction of the slowest side by "skidding". The frame of such a vehicle must be strong and rigid to withstand the forces that the steering mechanism creates.

The advantages of skid-steering are that it quickly can change the orientation of the vehicle, and that it has good manoeuvrability. The low mechanical complexity makes it a low cost solution, and its robustness and traction capabilities make it suitable for rough terrain. On the other side; Steering performance strongly depends on the surface it operates on, and it offers poor accuracy. It is also complex to model mathematically because the "skidding" varies with the surface and the speed of the vehicle, see Golconda [2005]. Wear and tear on the wheels is also high under turning and it damages the surface during steering. And since the surface in this context is arable land, this steering scheme might damage valuable crop.

The steering system with tracks are found in excavators, military tanks and tractors, as shown in figure 6.1 on page 50. Wheeled version of this steering is often found on skid-steer loaders, military robots and on small mobile robot platforms.

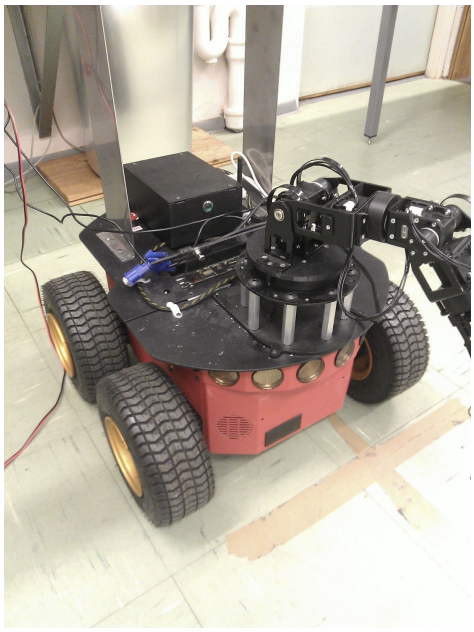

Figure 3.1: Pioneer *P3-AT MOBILE ROBOTS* skid steered mobile platform with 7 degrees of freedom manipulator used for haptic control algorithm research at NMBU.

3.2 Frame Articulated Steering

According to [Holm, 1970] articulated means jointed or segmented. An articulated steered vehicle has two or more frame units jointed together, and they should be an integral part of the vehicle. The joint(s) connecting the frame parts together, has a maximum of three degrees of freedom, and they are yaw, pitch and roll. This steering system normally uses all wheels to propulsion the vehicle forward.

The advantages of articulated steering is it's high mobility in difficult terrain, and it makes operation in narrow aisles easier, see [Toyata, 2014]. The mechanical complexity is also low and the control complexity is also lower than skid steering, and it offers good steering accuracies. If differentials are used, it gentle against the surface it steers on, while at the same time losing some traction. The negative aspects of articulated steering are added frame complexity, and that zero turning radius is not possible.

The steering is usually realized by hydraulically actuated cylinders that turn the joint(s) towards the side the vehicle is steering away from. Such steering is found in wide range of terrain going vehicles spanning from small lawn mowers, to heavy duty dumpers, and has become more or less the

standard in forestry machines.

Figure 3.2: Articulated steered modern Case IH STX 530 Quadtrac at the Maldon Working day 2011, courtesy tractors.wikia.com.

3.3 Four Wheel Steering

In four wheel steering (4WS), each wheel is articulated to the desired heading and the front and back wheels are out of phase and this gives four wheel steered vehicles a smaller turning radius compared to a similar sized vehicle with conventional two wheel steering. The issues of such a design are actuation complexity, and the high accuracy needed in the coordination control, and the advantages are very good manoeuvrability in unprepared terrain, see [Shamah et al., 2001] and [Kelly, 2010].

Crab Steering is a common variation of four wheel steering where the orientation of the vehicle is locked, and all wheels operate at the same speed and point in the same direction. No other steering schemes support this feature.

There are several ways to implement 4WS, and one way is to use a large linkage system that synchronizes the front and rear wheels separate whilst maintaining the anti-symmetry between the front and back wheel from one actuating point. Another solution is to individually actuate each wheel, and make the synchronization in a pc/micro-controller. The mathematics and geometry of this approach is discussed further in section 7 on page 63.

Vehicles that use this steering regime are mobile agricultural robots, see for example Bonirob in figure 2.5 on page 13, and some tractors design. This steering seems to be an early standard in mobile agricultural robots.

Figure 3.3: Four wheel steered Seekur is a all-weather, outdoor robot platform for outdoor research, courtesy Adept MobileRobots

3.4 Steering Evaluation

The steering decision can now be done, and we start with the most important parameter, accuracy, as the NMBU Mobile robot is intended for precision farming were demands for accuracy is high. As shown in table 3.1 on the next page all steering schemes provides this. The next aspect is manoeuvrability, and it is important for minimizing head land area and the associated costs in both time and energy. Here skid steering and four wheel steering is better than articulated steering because they can achieve zero turning radius. Surface damage is the next element in the list, and it can be detrimental for newly planted crops, and this makes skid steering undesirable. Another import design feature on our robot is that it should have the tool inside the frame, and preferable the tool's center of mass should coincide with the robots center of mass to ensure equal normal force on each wheel for maximal traction capabilities. Also the volume of free space inside the robot should be as high as possible, and since frame articulated steering has its actuating joint inside the frame, this configuration steals valuable volume. Power consumption is important on an autonomous vehicle, and as shown in table 3.1 on the facing page this puts the last nail in the coffin for skid steering. The last detail we want to interpret in our robot design is Crab Steering, and since four wheel steering is the only steering scheme that supports this quality, it is chosen on our NMBU mobile robot.

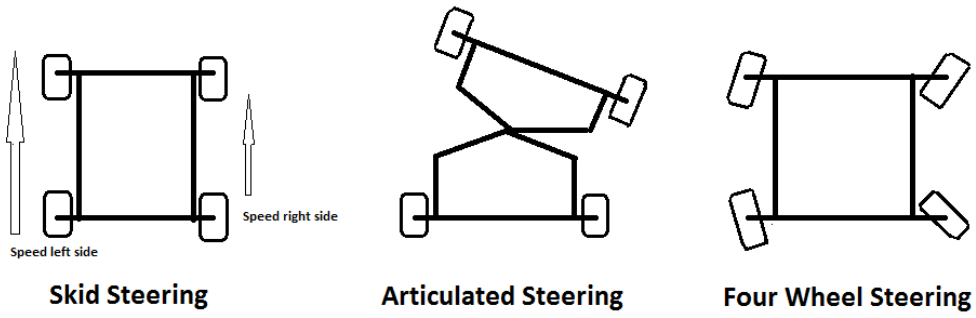

Figure 3.4: Shows the different steering schemes evaluated for the NMBU mobile robot in a right turn.

	Skid Steering	**Articulated Steering**	**Four Wheel Steering**
Accuracy	Medium/High	Medium/High	High
Manoeuvrability	High	Medium	High
Surface damage	High	Medium/Low	Low
Volume inside robot	High	Bad	High
Power consumption	High	Low/Medium	Low
Crab Steering	No	No	Yes
Mechanical Complexity	Low	Low	Medium
Robustness	High	High	Medium
Control Complexity	Low	Medium	Low
Number of actuated joints	0	1	4
Cost	Low	Medium	Medium/High

Table 3.1: A table similar like the one used in [Shamah et al., 2001] is used for steering system evaluation. This table lists the most important topics for our robot at the top, and then gradually presenting less important features further down.

3.5 Steering Components

It is becoming more and more normal to have separately actuating components, see Bjerknes [2012], rather than large linkage systems. The reason for these are numerous but one of the main reasons is the increased complexity that rules out larger linkage systems. Also mathematical model are easier to follow with individually actuated joints, see section 7 on page 63, and the flexibility of such system meets today's high standards.

Since our robot is electric we found out that hydraulically actuated joints would only introduce delay, increase complexity and reduce efficiency, and the solution is to have electrically actuated joints. Normally such rotating joints are served by a servo motor and this is solution that the author has seen the benefits of live, see Bjerknes [2012].

Figure 3.5: An exploded view of the steering components [Blomberg, 2014].

3.5.1 Electric Servomotors

> "A Servo Motor is defined as an automatic device that uses an error-correction routine to correct its motion. The term servo can be applied to systems other than a Servo Motor; systems that use a feedback mechanism such as an encoder or other feedback device

> to control the motion parameters. Typically when the term servo is used it applies to a 'Servo Motor' but is also used as a general control term, meaning that a feedback loop is used to position an item." [Anaheimautomation, 2013]

They are often found in industrial applications were precise operations are needed and are generally more expensive than a stepper motor that can be used for simpler, yet similar tasks [Anaheimautomation, 2013].

There are two main types of electric motors on the market today, and the cheapest and easiest to control are brushed motors that has shorter lifespan and poorer efficiency than brush-less motors, that delivers more torque at low speeds and requires more sophisticated motor controllers. In our robot design we chose brush-less motors to save weight and have good low rpm torque.

An expensive technology becoming more and more popular is integrated servomotors, and the idea here is to add simplicity in the physical set-up of the motor and motor controller by *integrating* the motor controller inside the motor making them one unit. This reduces volume and offers better protection to the servo system as fewer connections are needed. The control of such a system can be described more like plug and play compared to separate components, as described in section 5.1.4 on page 46.

Integrated servomotor

The motor that were chosen is a Danish high end brush-less integrated JVL MAC 141 servo motor of 134 Watts, capable of delivering 0.48 nm nominal and 1.59 nm peak torque [JVL Datasheet, 2014]. It is fitted with an CANopen communication protocol interface, MAC00-FC4, with m12 industrial connectors to receive and send messages over the CAN bus-cable, via the PEAK CAN-USB adapter, connected to the laptop that runs the Robot Operating System *ROS Hydro Medusa*.

The mode that servo motors is going to operate in is called position mode and more information on this mode is found in JVL Manual [2014]. In this mode the servo motors follows the commended positions from ROS, which is running the Ackerman equations found in section 7.6 on page 75, and if a servomotor senses that it isn't moving according to the commanded position, it will apply force to get in the correct position.

3.5.2 Reduction Gears

The steering torque needed to operate the steering system varies much, and the best solution would have been to do field tests, that identified the needed

(a) The *Integrated JVL MAC 141* 134 watts servo motor chosen for our mobile agricultural robot.

(b) The *APEX DYNAMICS AB060* two stage planetary gear with 60:1 ratio chosen for the servo motors.

Figure 3.6: Some of the mechanical components used in the steering system.

torque to turn the wheels of the robot under different conditions, but the climate in Norway at this stage didn't allow for this. Instead a similar method to Madsen and Jakobsen [2001] is used, were one assumes that the wheel is stationary on dry concrete, and then uses a simple formula to calculate the needed torque to turn the wheel, see Grimstad [2014] for more details.

Obliviously the lowest steering torque demand is present when the robot is moving on hard surface, and the highest steering torque demand is when the robot is stand still situated in deep mud. Since our robot is likely to operate in both conditions, and by including the fact that efficiency goes down if gear ratio is increased, we must find a gear ratio and gear efficiency that gives us fast enough steering rate, while at the same time offering high enough torque. Since the servo motor is capable of delivering three times the nominal torque under a short period, see section 3.5.1 on the preceding page, the muddy conditions will be covered by this feature.

Worm Gears

Worm gears are cheap and readily available, and they can be be delivered in a wide range of gear ratio. They can be advantageous if a 90 degree bend on the gear is needed and there is limited space. The downsides of these gears are their efficiency, and it is not uncommon that it is under 50%. This is undesirable on the robot if the steering system is activated often, as precious battery energy is transferred to heat via friction. Another feature of gears in general is that they are self locking if efficiency is 50 % or under SEW-EURODRIVE [2014], this means that the gear can hold the same torque that it can provide. Self locking worm gears are used in the *Mobile Robot for Weeding* shown infigure 2.5 on page 13 and Madsen and Jakobsen [2001] reported problems with this feature.

Planetary Gear

Planetary gear, also called Epicyclic gear, are regarded as one of the most efficient gear types according to [SEW-EURODRIVE, 2014]. They can be delivered in one stage or multi stage, where the later is several planetary gears stacked together to increase gear ratio. They are also significant lighter than a similar worm gear.

A *APEX DYNAMICS AB060* two stage planetary gear with 60:1 ratio is chosen for the NMBU mobile robot. This gear has efficiency of >94% according to Grimstad [2014], and will mounted directly above steering axle under servo motor. This gives us nominal steering torque of $0.48nm \times 60 \times 0.94 = 27nm$ and a peak steering torque of $1.59nm \times 60 \times 0.94 = 90nm$.

Remarks

The steering components presented in section 3.5 on page 28, form a steering actuator system which we believe is *state of the art* at the moment, and the reason for this is that the components gives us a low volume, small footprint, high efficiency, high precision, high torque, coaxial steering actuator.

3.6 Encoders and Absolute Position

Since the steering system consist of four coordinated and individually actuated joints, we need something to measure absolute position in each joint, and the components capable of such a task are presented briefly in this section.

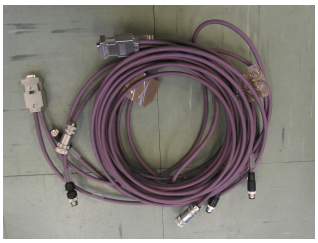

(a) CAN bus-cable custom made for our robot that all the motor controllers and the laptop is connected to.

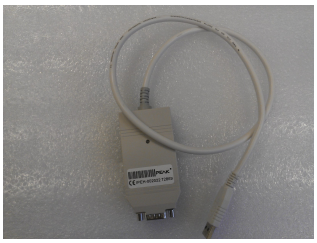

(b) *PEAK CAN-USB adapter* that provides the connection between the laptop and the CAN bus-cable.

(c) The 24 volt inductive sensor chosen for absolute position measurements of the steering axle.

Figure 3.7: Some of the control components used in the steering system.

3.6.1 Incremental Encoder

An incremental encoder is a rotary feedback device that is mounted to the motor to measure relative orientation and velocity. The most common types are optical and magnetic, whereas optical encoders typically offers greater resolution, and magnetic encoders are more robust [Anaheimautomation, 2014].

Inductive Sensor

Inductive sensor is a proximity device that detects metal objects contact-less, they are known for long operating life and robustness [Sick, 2014]. Every time the robot losses power, zero search is needed prior operating if dual supply is deactivated, see section 3.6.1 on the next page, to ensure that the absolute orientation of all wheels are known to the robot. The zero search is described by detail in JVL Manual [2014]. In short JVL offer two modes when using an external sensor, one is faster and less accurate, called *sensor type 1*, where zero is found by moving the steering axle clock wise to the inductive sensor is activated the first time, and set this point as zero. The other mode, called *sensor type 2*, is a bit slower and more accurate. Here the steering also moves clock wise to the inductive sensor is activated, but after the sensor is activated, the direction of movement is reversed and the point at which the sensor is disabled is defined as zero.

Torque Zero search

This type of zero search is described in JVL Manual [2014], and the essence of it applied on our robot is that the steering axles should move in predefined

direction after a start up, until it collides with a purpose built mechanical barrier. The point where the motor torque reach a specified value, pre-set as *Zero Search Torque*, is defined as the zero position.

The advantages of such a system are simplicity, as no external sensor is needed, and this makes it the cheapest option as well. Disadvantages arise from the fact that different surfaces has different torque demands, which results in different torque demand. This can lead to that the motor controller falsely believe that it has hit the mechanical barrier, say if the robot is started up in deep mud, or one wheel is stuck for other reasons. The result is that the absolute orientation of the wheel(s) is unknown. Another possible pitfall is that foreign objects like mud, roots and stones can habitat the mechanical barrier, and when the zero search mode is activated, the steering axle will collide in the foreign objects, rather than the mechanical barrier and thereby cause a faulty zero position.

Dual Supply

JVL has a feature they call dual supply, see JVL Datasheet [2014], and in short it is a extra power supply, feed from separate battery, only for the motor controllers, that keeps the control circuitry active so that absolute orientation can be maintained under a power loss. This will significantly reduce the amount of zero searches needed on our robot, but also add weight and complexity.

3.6.2 Absolute Encoders

Absolute encoders has the same features as incremental encoders. In addition they retain position information even when they are powered off thereby eliminating the need to perform zero search during a start up. The disadvantages are higher cost than incremental encoders.

Single Turn

Absolute single turn encoders specify the absolute position within one turn of the shaft. When 360 degrees of measuring range is covered, it starts to count from the beginning again, [Deemencoders, 2014]. A single turn encoder cannot be used in our steering servo motor since we have a planetary gear mounted to it. The reason for this is that the single turn encoder only will track the motor position within one turn, and not the planetary gear. The only place it can be mounted is after the planetary gear, then it correctly can track the absolute orientation of the steering wheel.

Multi Turn

Absolute multi turn encoder has the same features as absolute single turn encoders, except that it can count the number of revolution it has travelled. [Deemencoders, 2014]. This encoder type can be mounted directly to our servo motor to track the absolute orientation of the steering wheel.

3.6.3 Practical Implementation

We use the built in incremental encoder in the servo motor with a m12 sized 24 volt inductive sensor for absolute orientation of the steering wheels using the *sensor type 2*. As explained in table 7.1 on page 64 each wheel is free to rotate from 15° to 345° with 180° being the direction when the robot moves straight forward. In order to make this system robust the inductive sensor is going to placed near the mechanical stop at 15°. The placement and width of the metal plate that the inductive sensor is going to sense, ensures that there will never be a collision from the wheel hitting the mechanical barrier, or faulty zero search sequence.

Worst case scenario

Lets assume the worst case scenario, where one or more wheels are turned clockwise, while the robot is connected from its batteries, all the way to the mechanical barrier, so that the inductive sensor is facing the metal plate. We then power up the robot and by using *sensor type 2 zero search*, this should cause the motor controller to understand that the inductive sensor is activated, and then move the steering axle counter clock wise until the sensor is deactivated and set this point as zero.

If for some reason the motor controller needs to start this sequence with the inductive sensor deactivated, we will need to run a start-up script prior the zero search mode. This script would have to check whether the inductive sensor is activated or not, and if activated it should turn the steering axle a predefined number of degrees counter clockwise to ensure that the sensor is completely disabled and then start the zero search procedure. If the inductive sensor is found deactivated during this start-up script, the zero search should start immediately.

Chapter 4

Energy source for NMBU Mobile Robot

Rechargeable battery pack is the preferred our energy source on the vehicle. The reason for this is that the robot should have zero carbon dioxide emissions whilst operating[1]. This decision was made early in the process, see table 2.4 on page 18 and It seems like this is the way the vehicle industry are moving. The mobile robot industry has been in this world for decades. Electricity makes controlling the vehicle easier and hence most robots are electric.

4.1 Specific Energy

We have just under 3 kWh of energy on our robot, this quite much for such a light design. The down side of batteries is that the don't contain much energy compared to gasoline, due to their low specific energy. Diesel has a energy density of $10.1 kWh/litre$, see [Energilink-TU, 2008] and a specific energy of $12.0 kWh/kg$. This might be a issue later in the project if power demanding operations like tillage is a wanted operation for NMBU mobile robot. There are workarounds for this problem, namely diesel-electric system and a mobile agricultural robot that uses this technology can be found in section 2.5.1 on page 14, the down side of this solution is the increased complexity of the electro mechanical system and the added weight.

[1]There is always the discussion about carbon dioxide emissions during productions of batteries, but as far as the author know, no consensus on this subject is established

4.2 Lithium Batteries

There is a uniform agreement today that if you are going to power your vehicle with batteries, you should choose some type of Lithium technology. Lithium is the lightest of all metals, it actually floats on water. A key benefit is that it has the greatest electrochemical potential, and that makes it to one of the most reactive metal found. These properties makes it possible to achieve high energy and power densities, which is useful in high power applications like electric vehicle[Lawson, 2014].

Material Cathode	**Voltage of cell**	**Specific energy**	**Energy density**	**Thermal stability**
Cobalt Oxide	3.7 V	0.195 kWh/kg	0.560 kWh/litre	Poor
Nickel Cobalt Aluminium Oxide	3.6 V	0.220 kWh/kg	0.600 kWh/litre	Fair
Nickel Cobalt Manganese Oxide	3.6 V	0.205 kWh/kg	0.580 kWh/litre	Fair
Manganese Oxide	3.9 V	0.150 kWh/kg	0.420 kWh/litre	Good
Iron Phosphate	3.2 V	0.100 kWh/kg	0.333 kWh/litre	Very good

Table 4.1: This table gives a comparison of different Lithium Ion Cathodes used With carbon Anodes [Lawson, 2014].

4.2.1 State of the art

Lithium batteries cells from Panasonic used in Tesla model S, has according to this source [Tesla, 2011] a specific energy of $0.25kWh/kg$. This is roughly 40 times less specific energy than diesel.

The Panasonic battery cells used in Tesla motor needs a cooling unit, a control system and a casing when used in the car, this is according to [Tesla, 2011] one third of the total weight of the battery. Specific energy for Tesla motor's battery pack becomes roughly $0.17kWh/kg$.

Like wise the diesel need a tank to contain the fuel and some safety implements to be stored in the car, for simplicity lets assume that this also weighs one third of the total weight of the diesel system found in cars. Specific energy for the diesel system becomes $8.0kWh/kg$. This gives the diesel system 47 times higher specific energy density.

In comparison, the battery on the NMBU mobile robot has a specific energy of $0.08kWh/kg$, this 100 times less than a diesel system.

4.2.2 $LiFePO_4$ Technology

Phosphate based technology has superior thermal and chemical stability. This yields a better safety characteristic than other Lithium-Ion technologies that uses different cathode materials. Lithium phosphate cells are robust to misuse during charging and discharging and are said to be incombustible in the previous events. They are more stable during overcharge or short circuit conditions, and has the ability to withstand high temperatures. Phosphate chemistry also offers long cycle life, typically up to 2000 cycles [Lawson, 2014] The downside of this technology is lower energy density compared to high density Lithium technology like Nickel Cobalt Aluminium Oxide. However the NMBU Mobile Robot is a prototype where the main concern is safety, and lower energy density is not a problem in this phase of the project.

4.3 Battery for NMBU Mobile Robot

The battery technology and a suitable product was chosen quickly in Brazil as this was suppose to be an easy component to decide, and given this projects short time frame, everything that could be decided quickly were decided quickly. So we ended up buying batteries from Golden Motor, located in China. Later on in the project this tactic revealed it's drawbacks, one of them are mentioned in section 4.6 on page 42 and the other one is described in figure 4.2 on page 41. A third surprise is described more in detail in section 4.4.1 on page 39 and has nothing to do with the battery itself, rather with our lack of understanding that one cannot automatically assume that a 48 volt battery will work on a 48 volt integrated servomotor.

The good thing about the batteries, is their price per kWh, and it is important to have enough energy to carry out large scale field testing. Also since battery technology is done a lot of research on nowadays, it would be clever to dedicate a whole master thesis on optimum battery packs for NMBU mobile robot in near future, to solve the a aforementioned issues. Battery chosen for the NMBU mobile robot weighs 18 kg and has 1.5 KWH of energy

per battery.

(a) The model LFP-48V30M, is the chosen battery system for NMBU Mobile Robot.

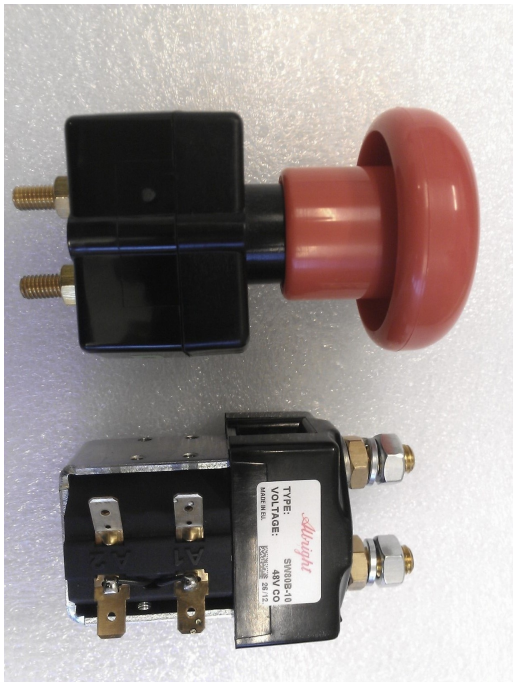

(b) The emergency stop button and main solenoid contactor chosen for NMBU Mobile Robot

Figure 4.1: Energy components.

4.4 Faulty wiring from supplier created short circuit

Golden motor has delivered two battery packs for NMBU Mobile Robot. When the first battery pack was coupled to the charger, smoke came out of the XLR-connection, and the connection were immediately disconnected by us.

Multimeter test showed that the wiring on the battery XLR-connection was different, than the charger XLR-Connection. More specifically, battery XLR-connection has pin 1(+) and pin 3 connected together, and pin 2(-) separate, as shown in figure 4.2c on page 41. Whereas charger XLR-connection has pin 2(-) and pin 3 connected together, and pin 1(+) separate, shown in figure 4.2d on page 41

The aforementioned produced a bridge between positive a negative poles on the battery, and this created the short circuit that produced the smoke. Damages to the connections are shown in figure 4.2a on page 41 and figure 4.2b on page 41

The multimeter test revealed that the charger pin assignment follows the industry standard of XLR-chargers, namely pin 1(+), pin 2(-) and pin 3 coupled to pin 2. It also showed that the battery does not follow the industry standard. This fault is something we didn't expect, and the setback in time for our robot project, was very undesirable. A well documented e-mail was sent to China, but they wouldn't reply. Luckily the other battery was correctly wired.

4.4.1 Actual voltage of 48 Volt $LiFePO_4$ battery pack

A 48 volt battery system is made up of four 12 volts battery connected in series, the 12 volt battery system is realized by connecting four 3 volts cells serial, see [Lervik, 2014] However the actual voltage in a 3 volt $LiFePO_4$ cell is nominally 3.3 Volt, and this leads to nominal voltage of 52.8 volt as shown in figure 4.2c on page 41. The maximum voltage a single $LiFePO_4$ cell can have is 3.65 Volt according to [Lervik, 2014], and in a 48 volt(16 cell system) this translates to 58.4 volt[2] . A proof of this is shown in figure 4.2d on page 41 were the charger outputs 58.4 volt.

4.4.2 Battery formulas

Batteries are usually labelled with it's ampere hours and voltage, from that information, energy can be calculated readily in various format.

Kilowatt hours

$$kWh = \frac{Ah \times V}{1000} \tag{4.1}$$

Kilojoule

$$kJ = 3.6 \times Ah \times V \tag{4.2}$$

[2]Its normal practice that the battery cell is charged up to 3.6 volts[Lervik, 2014] , given a total of 57.6 volt for this 16 cell system, as the charger side need a slightly higher voltage to keep the current in the batteries(!)

Equivalent litres of Diesel

$$Litre_{Diesel} = \frac{3.6 \times Ah \times V}{10.1} \tag{4.3}$$

Equivalent kilograms of Diesel

$$Kg_{Diesel} = \frac{3.6 \times Ah \times V \times 0.84}{10.1} \tag{4.4}$$

Burn time

$$Bt_h = \frac{kWh}{kW_{av}} \tag{4.5}$$

(a) Shows the damaged battery XLR-plug

(b) Shows the damaged charger XLR-plug

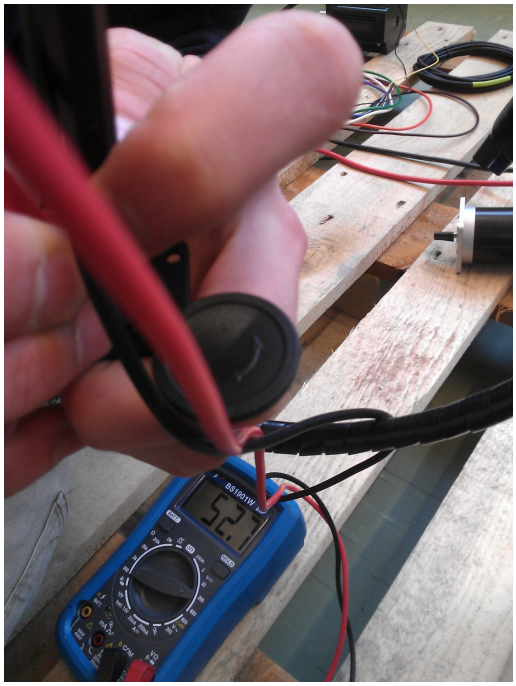

(c) Shows that battery XLR-connection has pin 1(+) and pin 3 connected together, and pin 2(-) separate

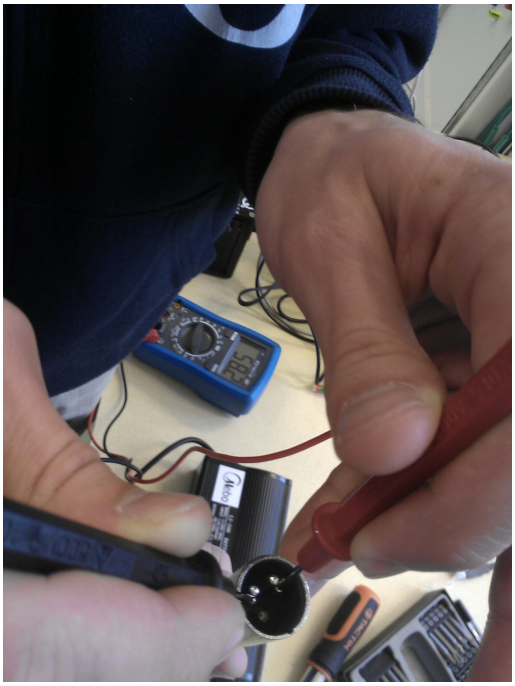

(d) Shows that charger XLR-connection has pin 2(-) and pin 3 connected together, and pin 1(+) separate

Figure 4.2: Faulty wiring on the battery created a short circuit when connecting battery to the charger

4.5 Battery change

There will be a need for changing the batteries during operation in the future. The robot should be able to do this battery change by it's own, and the slang term for this feature is "hot-swappable batteries". What it means in practice is that there is no loss of power or function to the robot, if one battery is removed and replaced. Then the robot can use a on-board manipulator to change it's batteries. This is one of the main reasons why we equipped the robot with two battery packs.

This idea implies that the two batteries are connected together in parallel, and although each of the purchased batteries has it own BMS(Battery Management System)included, a separate BMS to control operation of the paralleled battery packs is needed. The reason for this is to avoid high current flow, caused by different battery potentials, going from the newly replaced battery to the battery waiting to be changed as this may be detrimental to the batteries, [Lawson, 2014].

4.6 Battery Managements Systems

There are many types of BMS, from simple versions that only provides fundamental protection to the battery, like the purchased Golden Motor battery packs shown in figure 4.1a on page 38, by avoiding "out of tolerance" operating conditions, to high end automotive BMS that keep track advanced features like, state of charge(SOC), state of health(SOH), range possible with the remaining charge in the battery, and emergency "Limp Home Mode" in case of cell failure.

4.7 Emergency Stop System on NMBU mobil robot

The two battery packs are connected to a main solenoid contactor each, which is normally open, meaning that without electricity present on the solenoid circuit of the contactor, no current passes trough the main circuit in the contactor. The the solenoid circuits of this contactors is supplied from battery in advance of the main solenoid contactor, from there it has to pass four emergency buttons connected in series before it finds ground. This means that if either of the four emergency buttons are pushed down, both main solenoid contactors are open, and the robot is killed.

Chapter 5

Propulsion

5.1 Propulsion Components

The first propulsion system we started to look at where geared hub motors, as they have been used in Madsen and Jakobsen [2001], and the problem that with most of them was that they where spinning to fast fast for our robot, making them to weak(torque) for our design. Another problem with the geared wheel hub motors was the unknown quality since they were cheap, and delivery time could be a problem from China. The closest we came to hub wheel motors that might work where intended for wheel barrow. The lack of flexibility made this option less desirable.

5.1.1 Propulsion Motor

After this first search for applicable motors done in Brazil, we quickly decided that brush-less dc(BLDC) motors was what we needed, and one reason for this that they offer a nearly flat torque curve from low rpm, meaning that the robot would operate nicely in low speed, which is necessary for certain operations.

Second option was a flat armature "pancake" motor from Germany, which provided enough torque, and met our quality concerns, but this company were not interested in us as customer. After this Lars Grimstad became responsible for this part of the project he contacted a local company *Electro Drives* in a city 45 min from our university, called Askim. They were interested in our project and after short meeting in Askim, they became our main supplier for motors and gears. The chosen motors is 600 w and has a nominal torque of 1.32 nm [Grimstad, 2014] and are shown in figure 5.2b on page 45.

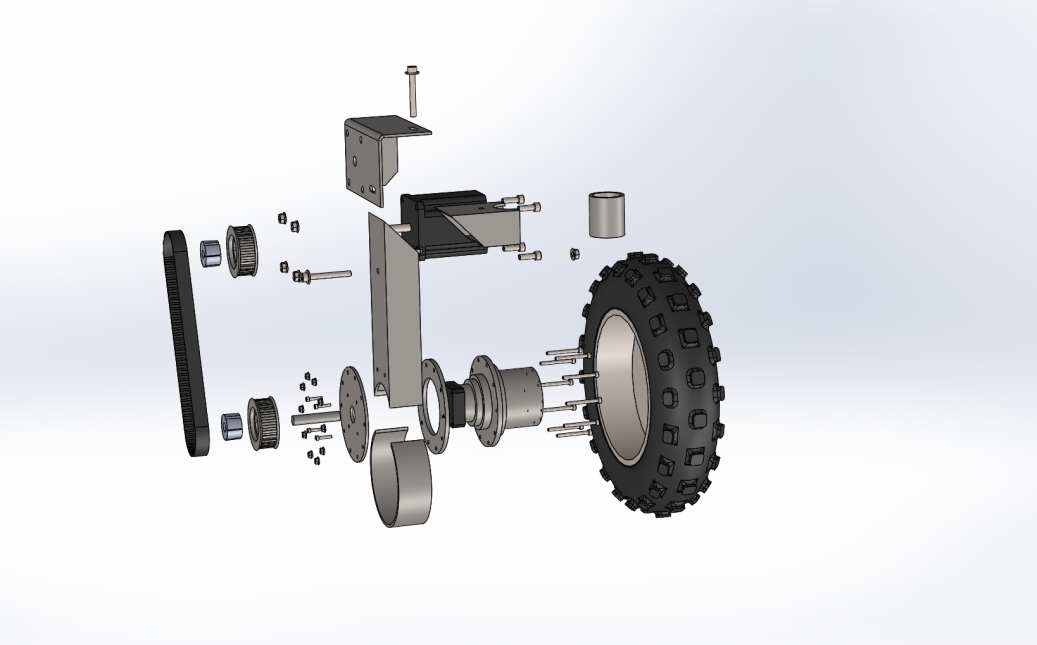

Figure 5.1: An exploded view of the propulsion components.[Blomberg, 2014]

5.1.2 Reduction Gear

Planetary gears were chosen for propulsion gearing because of their high efficiency, this discussed further in section 3.5.2 on page 29, and the chosen gear *Apex dynamics AL110* ratio 60 shown in figure 5.2a on the next page has a efficiency that is larger than 94 %. More deatails in this topic are given in Grimstad [2014]

5.1.3 Motor controller

The chosen motor controller is a brush-less dc *HBL2360* from Roboteq. It has two channels, meaning that one controller is capable of controlling two motors forward and reverse, and our two Roboteq controllers are going to power one side each. The maximum voltage input is 60 Volts, delivering 50 ampere continuous and 75 ampere peak, per channel and uses heat sinks for cooling,[Roboteq, 2013]

It supports CANopen communication protocol which we use for communication and has USB connection for easy set-up by pc. Support for Micro Basic Scripting is provided, which mean that we can write small programs executable in the controller, and thereby assign low level tasks for decentralization. The mode that the propulsion motors should operate in is called

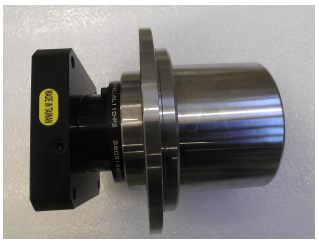

(a) The chosen two stage planetary 60:1 reduction gear *APEX DYNAMICS AL110*

(b) The chosen propulsion motor *BL823-A0K* from 3MEN TECHNOLOGY in Taiwan

(c) The versatile *Roboteq HBL2360* motor controller for the propulsion motors

Figure 5.2: The main components of the propulsion system

closed loop speed mode, see [Roboteq, 2013]. Here the speed of the motors are given by the Ackerman equations, see section 7.6 on page 75, running in ROS. By implementing a PID loop inside the controller that uses the actual speed of the motor measured by hall sensors or encoder as input, the speed of the motors closely follows the commands sent from ROS

5.1.4 Practical Implementation

The chosen propulsion will the give a nominal torque τ_{pn} of

$$\tau_{pn} = 1.32nm \times 60 \times 0.94 \times 0.96 = 71.5nm \tag{5.1}$$

and conservatively a possible[1] estimated peak torque τ_{pp} of

$$\tau_{pp} = 71.5nm \times 3 = 214,5nm \tag{5.2}$$

Some even claims that BLDC motors can deliver brief peak torque up to four times the nominal torque. [Design, 2009]

Placement

First the motor were intended to be bolted on the gear box inside the wheel to maximize efficiency, but when the CAD drawing of this solution were available, they revealed a design issue that no one had thought about before. The problem was that the propulsion system pointed so far out of the wheel that it could be problem if the robot were operating in a area of sufficiently

[1] Although such moment are possible, currently our robot is limited to a peak torque around $1.5 \times \tau_{pn}$

high obstacles, like stones and roots. In addition to making the robot look weird, this solution would also compromise possible tool-working-width, and hence this solution were dismissed.

Tooth belt or timing belt were present as a workaround for this problem by [Grimstad, 2014], and the propulsion motors could be placed up in the frame, making only the planetary gear point out of the wheel and this made the robot look "healthy" again, and the aforementioned problems is greatly reduced. The cost of this solution is a slightly reduced efficiency, but [pfeiferindustries, 2014] reports a efficiency up to 98 % on toothed belts when properly installed, and this is acceptable on our robot. Chains were not considered in our design as they require regularly maintenance, and has poorer efficiency than toothed belt if not maintained [pfeiferindustries, 2014] properly, whereas toothed belt are virtually maintenance free. Toothed belt system are also lighter than similar chained systems [pfeiferindustries, 2014].

Hall sensors

In theory [Roboteq, 2013], setting up the propulsion motor and the Roboteq propulsion motor controller should be a trial and error procedure were there are six possible ways the wiring can be done either in the three hall sensor cables or in the three motor phase cables, and only one of them should give a nice operation both backwards and forward in both open and closed loop.

In real life however, we spent a lot of time trying to figure this out see figure 5.3 on the next page for fault searching. The reason for this time usage is one fault yet to be solved, that makes the motor operate nicely in closed loop speed mode forward, but makes the motor go unsteady in closed loop backwards and when operating in open loop, the motors moves nicely in both directions. This made us question our connections.

[Roboteq, 2013]

5.1.5 Encoder

Since the problem only occurs in closed loop speed mode backwards it is a problem when the hall sensor inside motor serves as feedback for speed. This is conformed on Roboteq's software Roborun showing a large error in the measured speed, resulting in the PID controller inside the Roboteq trying to correct this anomaly that doesn't exist, which makes the motor operate unsteady, as mentioned in section 5.1.4.

To correct this error we need good feed back, and one way to achieve this is by implementing a external incremental encoder in the propulsion system which will be mounted at the back of the motor. The encoder is

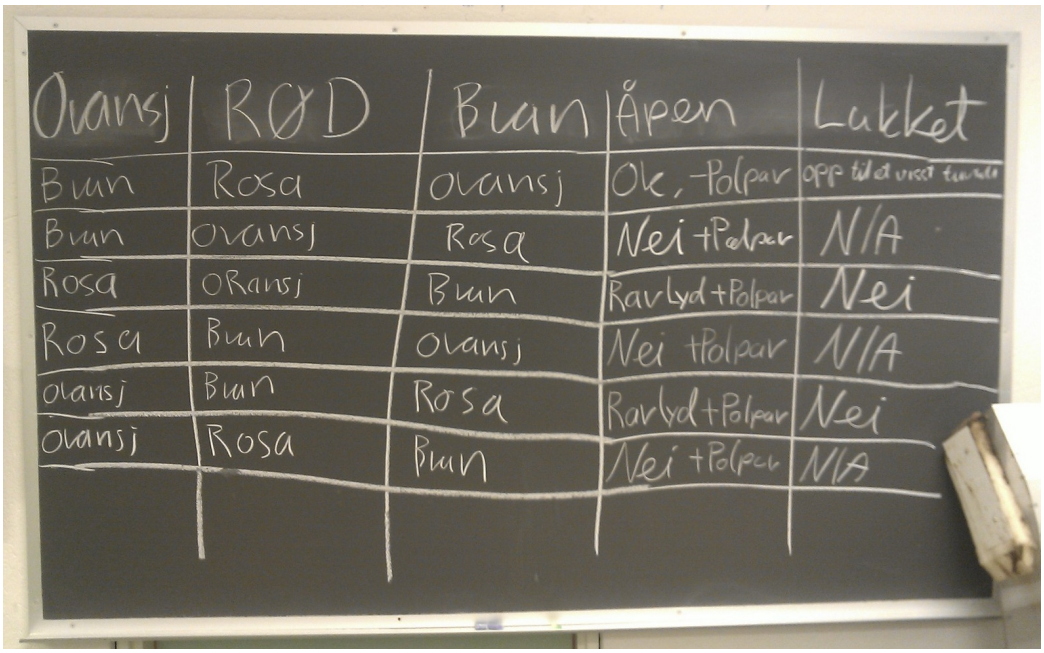

Figure 5.3: This figure shows the table we used to identify which one of the six possible hall sensors connections that were correct. The top row is the Roboteq's Norwegian color codes, the six row beneath are the color codes for the motor side and together they cover the six possible wirings. Number four from the bottom and the top one is the only one that worked in open loop, and since the top one is the only connection that was possible to run in closed loop mode, this is identified as correct.

then connected to the encoder inputs at the Roboteq motor controller and there by create a heavy duty servo system. For more detail regarding the propulsion components and calculations, see [Grimstad, 2014]

Chapter 6

Traction and Frame

6.1 Tracks versus wheels

Under the progress of building a Mobile Agricultural Robot hereby called vehicle, several choices have to be made, and one important decision is whether tracks or wheels are to be used.

One might think that tracks offer far better mobility than wheels and that if one intending to design a high mobility vehicle should use tracks. If a comparison between a six wheel rocker boggy and similar sized tracked vehicle is made, than there are only a few conditions that the tracked version is better[Sandin, 2003].They are

1. Terrain that is really soft like, loose sand, deep mud and soft powder snow

2. Obstacles(roots, stone) of a certain size that can get jammed between the wheels

3. Crevasses such as deep cracks in the ground, or on a glacier

6.1.1 Tracked vehicles

Application in daily daily life that supports these theories is snowmobiles and belt wagon are the preferred vehicle used in snowy areas. But in the similar conditions six wheels ATV are also used a lot. This higher mobility comes with some downsides, and that is greater complexity, and lower drive efficiency due to friction. But depending on the application it might be necessary with tracks.

Figure 6.1: Normally when ploughing, either the left or right wheel pair tracks the exposed furrow, and this amplifies soil compaction. The tractor shown above has both wheel pairs on the unploughed land, and this reduces soil compaction to some extent [Bjugstad, 2014]. A Caterpillar Challenger MT765B tracked tractor at work ploughing a field near to Leverton Lucasgate, Lincolnshire, Great Britain. The photo was taken on 22 October 2008.[Billinger, 2008].

The tracked vehicle is an old concept [Sandin, 2003], the first vehicles rolled out in early twentieth century, and in World War one they were extensively used. The basic design has not been changed since that is used to day on heavy equipment like excavators, bulldozer and so on. The configuration consists of a drive sprocket at one end, a idler wheel at the other end that usually also serves as a tension-er, and between the ends, something to support the tracks. The advantages of this design are that it is simple, robust and easy to control. This simple form has all the benefits mentioned above.

6.1.2 Advantages of tracks

Tracks have a continuous surface that is in contact with the ground this is the major advantage over wheels. A long belt with the same width as wheels puts a large surface on the ground, this yield lower ground pressure and travelling on softer ground becomes possible. Another benefit is that one get more treads or studs in the ground, and this gives better traction, and more pull/push force see figure 6.1 on the preceding page. The continuous surface between the front and the rear eliminates the problem that wheeled vehicles suffer from being high centred between the wheels. Also a correctly sized obstacle can get caught between the wheels on one side, but tracks always stay on top. The wheeled vehicle can get stuck in these situations, whereas a track would simply roll over the obstacle.

For our application this is not a problem[1] since our robot is going to operate under relatively smooth surfaces. The largest benefit of tracks versus wheeled vehicle is that the track can pass crevasses. It is possible to make a six or eight wheel vehicle to the job, but the complexity and cost goes in favour of the belts. Again this is not a problem for Mobile Agricultural Robot.

One way of getting some of the benefits of tracks with wheels is to lower the pressure in the wheels such that the tire is say one third flat. Then the area touching the ground is significantly larger and better performance on softer surfaces is achieved. The low speed ensures that the rubber does not get overheated due to friction.

6.1.3 Benefits of wheels

Wheels are more energy efficient than tracks, because of lower friction due to only one moving part. They are also more robust due to the aforementioned.

[1] Depending on how moist the ground is, amount of pull force needed, and the softness of the surface; vehicle with tracks may be the only solution. Later iterations of the robot might therefore include tracks

Wheels require little maintenance, and consist of few moving parts, perhaps only one wheel bearing. This makes a wheeled vehicle cheaper and easier to design, and all this are requirements for the NMBU Mobile Robot, table 2.4 on page 18

6.1.4 Wheels on NMBU mobile robot

Fredrik Meltzer, Lars Grimstad, and the author visited Røwde tires in Oslo, and the goal of this trip was to decide rims and tires for the NMBU mobile robot.

The main criteria given by frame designer Fredrik Blomberg was that the total wheel height had to be less or equal to 40 cm, see table 2.5 on page 18, so with this in mind several tires types and rims were auditioned. Fredrik Meltzer writes about tires in his master thesis, and his guidelines were followed.

There were five different candidates, the first tire that Røwde tires proposed shown as number four from the bottom in figure 6.2 on the facing page had low rolling resistance, and low traction, this was quickly dismissed as traction is important for this robot. The second tire shown as number two from the bottom in figure 6.2 on the next page had a bit more traction, and were evaluated further. The third tire proposed shown in the bottom of figure 6.2 on the facing page was a snowblower tire. According to Røwde, this was a tire they use to retrofit on lawn movers to increase climbing ability, and this tire seemed promising. The fourth tire shown as number three from the bottom in figure 6.2 on the next page had normal tractor tread, this qualified for traction purposes, but when measured, this tire was found to tall. The fifth tire shown on the top of the stack in figure 6.2 on the facing page was a bit wider and lower the the previous tires, this tire needed special rims, and it were found to small.

After this process were finished, two candidates were left, and the question was if traction were more important than rolling resistance on NMBU mobile robot, and since this robot should cope well with Norwegian conditions, the tire in the bottom of figure 6.2 on the next page is bought. For deeper coverage of traction science, see [Meltzer, 2014].

Figure 6.2: shows the five tires auditioned at Røwde AS for NMBU Mobile robot. Photo taken by the author.

Figure 6.3: Fredrik Meltzer to the left and Lars Grimstad to the right in the background when the chosen tire is mounted on the rim by Terje Thoresen. Photo taken by the author.

6.2 Frame

In my thesis I have assume that the frame were given, and this section briefly covers the authors sight on frame design in a practical way. For detailed presentation of the frame design process, see Blomberg [2014].

There is one major difference from other mobile agricultural robots, compared to our design, and that is the space allocated for the tool. The state of the art Bonirob, see figure 2.5a on page 13 has only a small space intended for the tool, and we have chosen to maximize the tool space in our robot, making it capable of performing light tasks done by traditional tractors today.

The size of the frame is based on that it should fit on a car hangar, and the dimensions are 1700 mm wide by 1100 mm long. It is made in part steel part aluminium, where the different metals are glued together for simple disassembly by heating the glue to to a temperature specified by the glue manufacturer. The suspension is passive consist of the natural flexibility found in the frame, and since arable land is generally smooth, this should be sufficient.

Tools should be mounted in the center of the frame, making the robot center of mass coincide with the tools center of mass, giving equal normal forces on each wheel assuming flat surface for optimum traction. When tool are not present in the robot, there will be a tool replica inside frame that gives lateral support to the robot. It is intended in the future that the robot should be able to change tool by it's own, and one proposal is to use linear actuators to lift and lower the frame to accommodate the change of different tool. For in depth coverage and fem analysis see Blomberg [2014]

Figure 6.4: This figure shows a rendering from SolidWorks of the frame shoving the tool replica as the triangle in the middle of the robot [Blomberg, 2014].

Part II

Independent Four Wheel Ackerman Steering

Summary part II

The main purpose of this master thesis is to develop kinematic equations for NMBU Mobile Agricultural Robot. The author's contribution to NMBU Mobile Agricultural is presented, and this proposal uses an inverse kinematics geometrical approach to find the kinematic solution. Kinematic constraints to NMBU Mobile Agricultural are identified, and we discuss whether dynamics can be neglected or not. Crab steering is steering scheme attainable with NMBU Mobile Agricultural, and we discuss the kinematics of such scheme briefly. Ackerman geometry is introduced, and four wheel Ackerman equations are derived for NMBU Mobile Agricultural.

Mathematical tools like curvature and turning radius is presented as input in kinematic equations, and a singularity workaround is presented. Four wheel Ackerman equations are developed further to give unambiguous steering angles for all steering wheel positions in NMBU Mobile Agricultural and separate equations for all four wheels are presented. A map from signed turning radius to local end-effectors is also included in the four wheel Ackerman equations, and this result gives us six unique kinematic equations. Input like signed turning radius and desired speed in center of robot output correct steering angle and speed of all four wheels.

Practical Implementation of kinematic equation is discussed, and a map from steering angles to number of motor turns is found, as well as a map from ground speed in center of robot to RPM in propulsion motors. Numerical singularity threshold in singularity workaround is also are discussed and found. An intuitive example where the robot follows a simple path is included.

In the end we present two proposals intended to minimize wheel slip when NMBU Mobile Agricultural Robot is operating in uneven terrain, and the relevance for these system in NMBU Mobile Agricultural Robot is discussed.

Chapter 7

Kinematic Model

The work presented in this chapter is the authors main contribution to the NMBU mobile robot. The motivation for this work is that the author could not find previous work that translated well to our mobile robot. The mathematics in this chapter are fairly simple, and it involves mainly geometrical relations and understandings.

Kelly [2010] have shown that all particles on a rigid body, moves in a manner instantaneously described as a solely rotation around a point called ICR (instantaneous center of rotation). The turning radius is defined as the distance between the vehicle center, and this instantaneous center of rotation (ICR).

The kinematic equations for our robot is presented in a geometrical form in this proposal, as the author believes this makes the kinematics easier to digest. It is however important to understand that the vector form is more commonly used as input in navigation task, but all the work presented below holds for vector form as well. Speed in center of robot and a tracked signed turning radius maps 1:1 to speed in x and y-direction and angular speed. The mapping from geometrical form to vector form is done by replacing R_t found in the equations in this chapter, with the right hand side of the following equation:

$$R_t = \frac{\sqrt{\dot{x}^2 + \dot{y}^2}}{\dot{\theta}} \tag{7.1}$$

And by replacing ground speed S with the right hand side of the following equation:

$$S = \sqrt{\dot{x}^2 + \dot{y}^2} \tag{7.2}$$

7.1 Inverse Kinematics

The model presented here is the inverse kinematics solution. From the steering radius we calculate the joint parameters needed to fulfil the steering radius, and they can seen upon as local end-effectors. They include the four independent steering shafts and the four individually controlled propulsion wheels. The global end-effector can here seen on as the system of local end effectors that provide the desired turning radius of the robot. The forward kinematics is of little interest for our model since we have eight actuators needed to work together by a solution found by the inverse method.

7.1.1 Kinematic Constraints

Constraint	From	To
Steering Angle	15°	345°
Steering Rate	0.1 $\frac{\circ}{s}$	270 $\frac{\circ}{s}$
Turning Radius	0 m	∞ m (straight line)
Wheel Speed	0.02 $\frac{m}{s}$	1.53 $\frac{m}{s}$

Table 7.1: This table show the kinematic constraint in the NMBU mobil robot, see section 7.6.2 on page 77 and section 7.5 on page 71 for more details

7.1.2 Dynamics

The Ackerman geometry only makes sense when speeds are low as it is a pure kinematic model, however our robot is operating at very low speed, below 5 kph under normal conditions, as shown in section 7.6 on page 75, and the associated dynamic effects become small. Steering actuators does not experience dynamic effect from the robot, as the wheels are centred under the steering actuators. Deviation from this simplification is taken care of by the high gain closed loop Roboteq motor controllers for the propulsion motors on the robot.

7.2 Crab Steering

Crab steering is a mode that is easy to implement, as each wheel turn exactly the same amount of degrees and has exactly the same speed, and the direction of the vehicle from straight line is the given by turning angle of the wheels. Assuming we have a known path to follow, then all wheel point in the direction of the instantaneous tangent at that particular point on the path. This wheel direction in degrees can be found by measuring the angle between the orientation heading and the tangent line. This steering mode may become useful if rapid change heading is needed, while at the same time maintaining constant orientation. Different operation on the field could also experience benefit from this steering mode. The kinematic equation for this mode is trivial and out side the scope of this thesis.

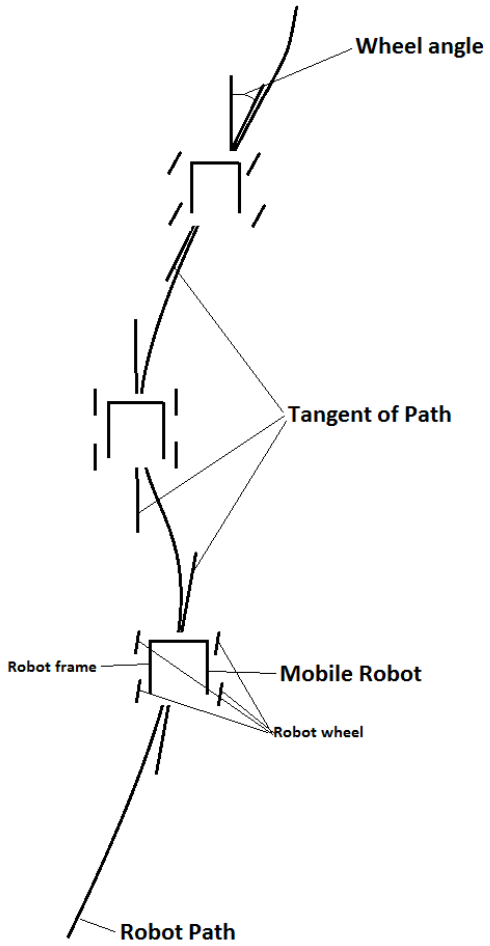

Figure 7.1: This figure shows how crab steering mode follows a path

7.3 Ackerman Geometry

Ackerman geometry is intended to avoid tyre slippage when following a curved path, see Norris [1906]. There are to types of Ackerman geometry, two wheel steering and four wheel steering. The former is often found in cars and tractors, and the key elements of such design are simplicity, and directional very stable. The latter is more seldom to see, but it offers several advantages over former, and perhaps the most important quality is reduced turning radius. It also reduces drive propulsion as the back wheels don't need to run over fresh terrain [Shamah et al., 2001]. Another important feature is that the front wheel and the rear wheel follows the same curves, this makes us certain that if the front of the robot can get round a corner, the back of

the robot can get round the same corner, given that the robot has the same width front and back.

There is no mechanical multi bar linkage solution that provide the Ackerman-conditions perfectly. It is possible to design linkage systems that works closely to the condition. Our choice of individually actuating each wheels steering, and wheel speed, merges the steering strength found in differential drive systems and energy efficiency of four wheel Ackerman steering. Another benefit of actuating each steering and propulsions motor is that the robot can follow the Ackerman-condition geometrically and mathematically perfect. This makes the robot capable of following a straight line, were *curvature* is zero, to turning in place were *steering radius* is zero. This gives us maximum mobility.

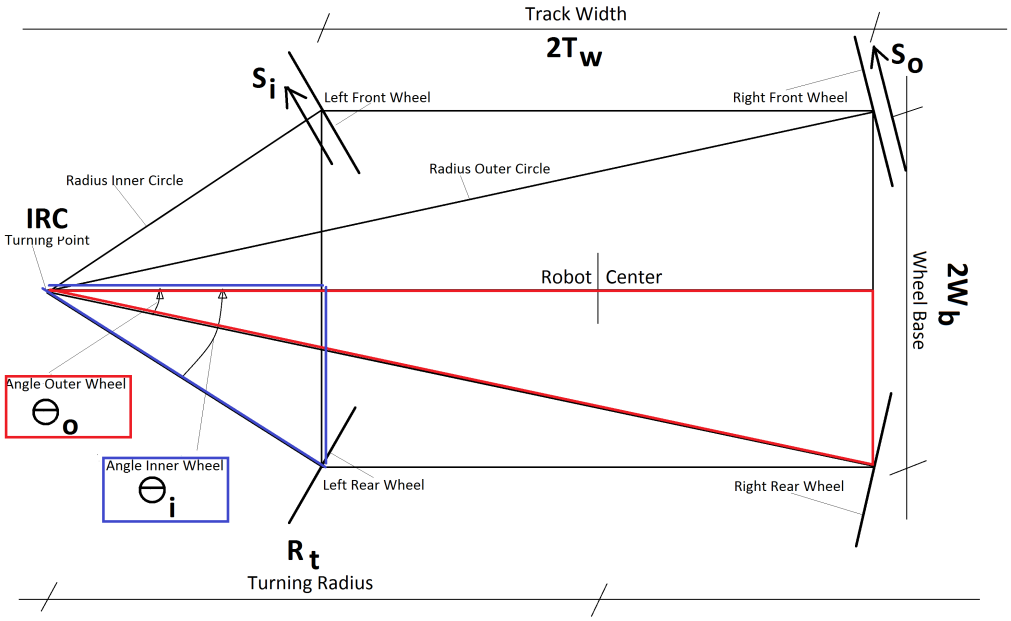

Figure 7.2: In this figure the four wheel Ackerman geometry is shown while the robot is making a left turn. It is from this figure that the equations presented in this chapter is derived from.

7.3.1 Four Wheel Ackerman Equations

Four wheel steering implies that the front right and rear right wheels follows a circle with larger radius, than front left and rear left wheels. Notice that this causes the steering angle of the inner wheels to be greater, than the steering

angle of the outer wheels, since the inner wheels follows a shorter radius then the outer wheels. This is easily shown in figure 7.2 on the preceding page. The later implies that the outer wheels has to spin faster than the inner wheels.

The basics in Ackerman geometry are very simple, you can get the correct angles by means of sine, cosine, and tangent. However one must by careful when selecting angular "tool", the author first auditioned tangent, and all went good until half the track width were input as turning radius. This is where nearby cathetus of inner wheel angle becomes zero and we have a singularity. The second candidate was cosine, and this turned out to be a better option than tangent, as the nearby cathetus becomes zero, arc-cosine reports 90°. Sine will also avoid the aforementioned singularity, but sine is a odd function and the author were uncertain if this feature could create problems when mirroring the robots left and right side, and when using the signed turning radius as steering input. Since cosine is a even function it is chosen.

The following abbreviations is used trough this chapter,

- Half track width is denoted by T_w
- Half wheel base length named W_b
- Turning Radius abbreviated R_t

Angle° Inner Wheel

The angle for the inner wheel, θ_i, is defined by the blue triangle in figure 7.2 on the previous page, where the nearby cathetus of this triangle is given by the turning radius minus half the track width, $R_t - T_w$, and the opposite cathetus is given as half the wheel base, W_b:

$$\theta_i = \arccos\left(\frac{R_t - T_w}{\sqrt{W_b^2 + (R_t - T_w)^2}}\right) \tag{7.3}$$

Angle° Outer Wheel

The angle for the outer wheel, θ_o, is defined by the red triangle in figure 7.2 on the preceding page, where the nearby cathetus of this triangle is given by the turning radius plus half the track width, $R_t + T_w$, and the opposite cathetus is still given as half the wheel base, W_b:

$$\theta_o = \arccos\left(\frac{R_t + T_w}{\sqrt{W_b^2 + (R_t + T_w)^2}}\right) \tag{7.4}$$

Since the robot can be regarded as rigid body, all parts of the robot experience the same angular velocity, and the well known relation, tangential speed is angular speed times radius $v = \omega \times r$ holds for the robot. Then the speed of the inner wheel S_i in percent with respect to the outer wheel is given by the distance from the inner wheel to the turning point ICR, divided by the outer wheels distance from the same turning point ICR:

Speed$\frac{m}{s}$ Inner Wheel

$$S_i = \left(\frac{\sqrt{W_b^2 + (R_t - T_w)^2}}{\sqrt{W_b^2 + (R_t + T_w)^2}}\right) \times 100\% \tag{7.5}$$

And hence the equation for the outer wheel with respect to the outer becomes trivial at this stage:

Speed$\frac{m}{s}$ Outer Wheel

$$S_o = \left(\frac{\sqrt{W_b^2 + (R_t + T_w)^2}}{\sqrt{W_b^2 + (R_t + T_w)^2}}\right) \times 100\% = 100\% \tag{7.6}$$

7.4 Curvature and Turning Radius

Curvature κ is the rate at which the tangential vector T turns per unit length, along the curve [Thomas et al., 2010] y that represents the path e.g $y = x^3$. It is common to use curvature when describing mobile robot kinematics Kelly [2010], and there are two version, the unsigned is shown here:

$$\kappa = \frac{|y''|}{(1 + y'^2)^{\frac{3}{2}}} \tag{7.7}$$

and the signed is shown below:

$$\kappa = \frac{y''}{(1 + y'^2)^{\frac{3}{2}}} \tag{7.8}$$

And it is this signed curvature that this proposal uses. The tangent vector gives us information about the local curvature in the plane, spanned out by the four wheels of the robot, in the three dimensional path. By choosing appropriate orientation of the curve, one obtain a rule that states; if the tangent vector rotates counter clockwise as the path goes forward, i.e a left turn, the curvature is positive. If the tangent vector rotates clock wise as the path goes forward, i.e a right turn, the curvature is negative. The local

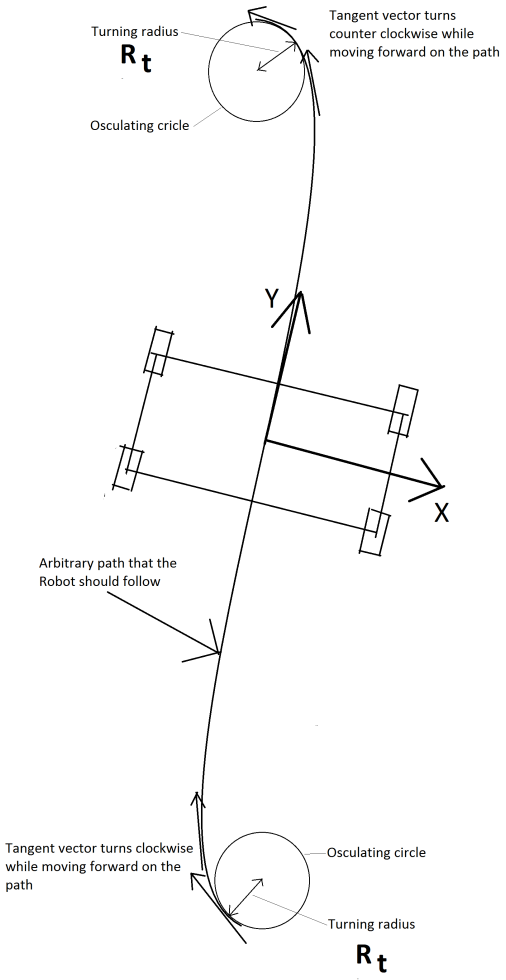

Figure 7.3: This figure shows a randomly chosen path that the Robot should follow.

radius of curvature, is the same as local turning radius, and the later is used in this thesis. R_t and curvature κ is closely related, namely:

$$R_t = \frac{1}{\kappa} \tag{7.9}$$

R_t is the radius of the osculating circle that most closely approximates the curve at the given point shown in figure 7.3, and radius of this osculating circle is the same as the steering radius needed for the robot to follow the path in that point, see figure 7.3. Since the turning radius is reciprocal to

the curvature, the sign of turning radius is also known and shown here:

$$R_t = \frac{(1 + y'^2)^{\frac{3}{2}}}{y''} \tag{7.10}$$

It is this information that is gives us unique steering angles for each wheel, and unique velocity of left and right side when following a path. This equations is presented in section 7.5.

7.4.1 Singularity Workaround

As seen in equation 7.10, there will be some conditions that will impose a singularity when calculating the needed turning radius, those are, but not limited to:

- When the path or curve is mathematical straight, as in one time differentiable, for example $y = x$, or a constant, fore example $y = 2$
- If x it self is zero, assuming that path is on the form $y = ax^b$

To avoid this singularity condition, we use a singularity test that calculates the curvature of the path y, e.g $y = x^3$, before the turning radius is calculated:

Singularity Test

$$\infty_t = \frac{y''}{(1 + y'^2)^{\frac{3}{2}}} \tag{7.11}$$

Since turning radius is reciprocal to the curvature, section 7.4 on page 69 the singularity condition in turning radius will be identified in the test, before it becomes a problem. If the test outputs zero, equation 7.10 will not be used as the path is straight, and all wheels will be commanded to 180° position and operate on the same speed, see figure 7.4 on the next page. If the test outputs anything else than zero, equation 7.10 will be used, and appropriate turning radius will be calculated.

7.5 Kinematic Equations

It is assumed that each wheel can rotate from 15° to 345° freely, with the area from 346° to 14° used as mechanical barrier, see figure 7.4 on the following page, to protect cables and other equipment from being torn apart. This design allows the robot to operate *continuously* from a straight line into a

left, or right turn, finishing off with spinning either counter clockwise or clockwise.

7.5.1 Unique steering angles

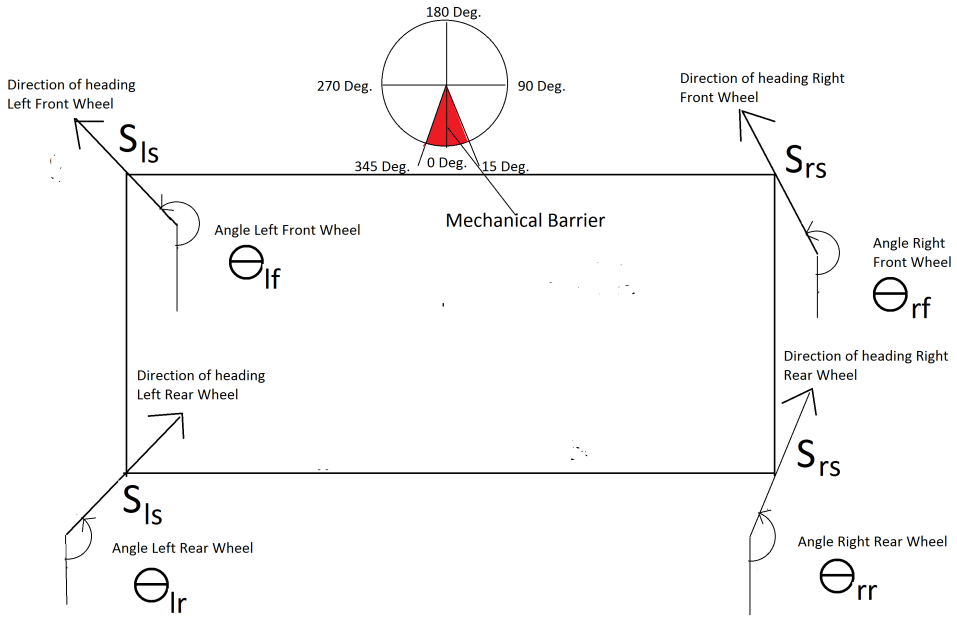

Figure 7.4: This figure shows each wheels individual steering angle in ° given from the same reference axis shown in the top middle of the figure. Note when driving straight forward all wheels are at 180°.

As seen in figure 7.4, all wheel are at position 180° when the robot driving straight forward, and the reason for this is that we want positive and unique angles for all possible positions of the wheel, to ensure that commands sent to the servomotors are unambiguous. This is solved including 180° in front the angle equations presented in section 7.3.1 on page 67, while keeping the speed equations untouched:

Angle° Inner Wheel

$$\theta_i = 180 + \arccos\left(\frac{R_t - T_w}{\sqrt{W_b^2 + (R_t - T_w)^2}}\right) \tag{7.12}$$

Angle° Outer Wheel

$$\theta_o = 180 + \arccos\left(\frac{R_t + T_w}{\sqrt{W_b^2 + (R_t + T_w)^2}}\right) \tag{7.13}$$

Speed$\frac{m}{s}$ Inner Wheel

$$S_i = \left(\frac{\sqrt{W_b^2 + (R_t - T_w)^2}}{\sqrt{W_b^2 + (R_t + T_w)^2}}\right) \times 100\% \tag{7.14}$$

Speed$\frac{m}{s}$ Outer Wheel

$$S_o = \left(\frac{\sqrt{W_b^2 + (R_t + T_w)^2}}{\sqrt{W_b^2 + (R_t + T_w)^2}}\right) \times 100\% = 100\% \tag{7.15}$$

7.5.2 Individual angle equations

We also need to make individual kinematic equations for the front wheels, and the rear wheels on each side, as they operate out of phase. This is done by setting a minus sign between the newly included 180° , and the angle equations found section 7.5.1 on the preceding page for the rear wheels, and plus sign for the front wheels. This action gives us one angle equation per wheel, while we still keeps the speed equations untouched:

Angle° Rear Inner Wheel

$$\theta_{ri} = 180 - \arccos\left(\frac{R_t - T_w}{\sqrt{W_b^2 + (R_t - T_w)^2}}\right) \tag{7.16}$$

Angle° Front Inner Wheel

$$\theta_{fi} = 180 + \arccos\left(\frac{R_t - T_w}{\sqrt{W_b^2 + (R_t - T_w)^2}}\right) \tag{7.17}$$

Angle° Rear Outer Wheel

$$\theta_{ro} = 180 - \arccos\left(\frac{R_t + T_w}{\sqrt{W_b^2 + (R_t + T_w)^2}}\right) \tag{7.18}$$

Angle° Front Outer Wheel

$$\theta_{fo} = 180 + \arccos\left(\frac{R_t + T_w}{\sqrt{W_b^2 + (R_t + T_w)^2}}\right) \tag{7.19}$$

Speed$\frac{m}{s}$ Inner Wheel

$$S_i = \left(\frac{\sqrt{W_b^2 + (R_t - T_w)^2}}{\sqrt{W_b^2 + (R_t + T_w)^2}}\right) \times 100\% \tag{7.20}$$

Speed$\frac{m}{s}$ Outer Wheel

$$S_o = \left(\frac{\sqrt{W_b^2 + (R_t + T_w)^2}}{\sqrt{W_b^2 + (R_t + T_w)^2}}\right) \times 100\% = 100\% \tag{7.21}$$

7.5.3 Mapping signed turning radius to local end-effectors

A map the from the signed turning radius to the robots local end effectors, explained in section 7.1 on page 64, are needed for the robot understand if it should turn to the left or right, when the signed turning radius is used as input. Definition of inner or outer side, changes when the robot is going from a left to right turn. As this definition is crucial to kinematic equations in section 7.3.1 on page 67, we make a simple sign changer that maps the current inner and outer side to correct kinematic equations:

$$C_s = \frac{R_t}{|R_t|} \tag{7.22}$$

and include it to all equations in section 7.5.2 on the preceding page, and the result is:

Angle° Left Rear Wheel

$$\theta_{lr} = 180^\circ - \frac{R_t}{|R_t|} \times \arccos\left(\frac{|R_t| - \frac{R_t}{|R_t|} \times T_w}{\sqrt{W_b^2 + (|R_t| - \frac{R_t}{|R_t|} \times T_w)^2}}\right) \tag{7.23}$$

Angle° Left Front Wheel

$$\theta_{lf} = 180^\circ + \frac{R_t}{|R_t|} \times \arccos\left(\frac{|R_t| - \frac{R_t}{|R_t|} \times T_w}{\sqrt{W_b^2 + (|R_t| - \frac{R_t}{|R_t|} \times T_w)^2}}\right) \tag{7.24}$$

Angle° Right Front Wheel

$$\theta_{rf} = 180^\circ + \frac{R_t}{|R_t|} \times \arccos\left(\frac{|R_t| + \frac{R_t}{|R_t|} \times T_w}{\sqrt{W_b^2 + (|R_t| + \frac{R_t}{|R_t|} \times T_w)^2}}\right) \tag{7.25}$$

Angle° Right Rear Wheel

$$\theta_{rr} = 180^\circ - \frac{R_t}{|R_t|} \times \arccos\left(\frac{|R_t| + \frac{R_t}{|R_t|} \times T_w}{\sqrt{W_b^2 + (|R_t| + \frac{R_t}{|R_t|} \times T_w)^2}}\right) \tag{7.26}$$

Wheel Speed% Left Side

$$S_{ls} = \left(\frac{\sqrt{W_b^2 + (|R_t| - \frac{R_t}{|R_t|} \times T_w)^2}}{\sqrt{W_b^2 + (|R_t| + \frac{R_t}{|R_t|} \times T_w)^2}}\right) \times 100\% \tag{7.27}$$

Wheel Speed% Right Side

$$S_{rs} = \left(\frac{\sqrt{W_b^2 + (|R_t| + \frac{R_t}{|R_t|} \times T_w)^2}}{\sqrt{W_b^2 + (|R_t| + \frac{R_t}{|R_t|} \times T_w)^2}}\right) \times 100\% \tag{7.28}$$

7.6 Practical Implementation of Steering

As mentioned previously, the robots four wheels spans out a local plane that the robot can move in. The path that the robot should follow is in three dimension. Since the robot can't dig into the ground, or fly, the z-axis coordinate will be followed automatically by the robot. Orthogonal projection(s) from the robots local plane, to a reference plane, is needed in order to translate the three dimensional path into the local path that the robot operates in. The mathematics behind this is fairly simple, and the topic will not be covered in this thesis.

Further the robot is assumed to know the path beforehand, i.e offline navigation. This path is generated by a three dimensional coverage path planning algorithm that accounts for hilly terrain, by ensuring equal distance between run overs in the local plane, thereby covering the field close to 100%.

There will be a device and/or algorithm, that extracts the *local* steering radius needed for the robot to follow the the three dimensional path. We further assume that if there is a deviation in where the robot should be, and it's actual whereabouts, a find back path is generated so the robot can continue it's task. The frequency of this position update will have to be determined during field test to reach the desired accuracy.

7.6.1 Numerical Singularity Threshold

In the numerical computer world, mathematical zero seldom occurs, and one need to specify a numerical threshold, that states that everything below a given value is defined as zero, see [Nielsen, 2014] and [From, 2014]. In our case, this will imply that when performing the the singularity test, there is a small range of absolute curvature, $|\infty_t|$, values that should state a singularity in the turning radius to avoid excessive calculation. To identify this small absolute singularity threshold, we briefly discuss the error that such a threshold introduce. First we identify that the precision for the robot needed under operation to operate satisfactory is e.g $\pm$ 2 cm. Lets further assume that the longest fields are e.g 2.5 km, and that the robot should be able to follow a straight line of this length with the desired precision, see figure 7.5

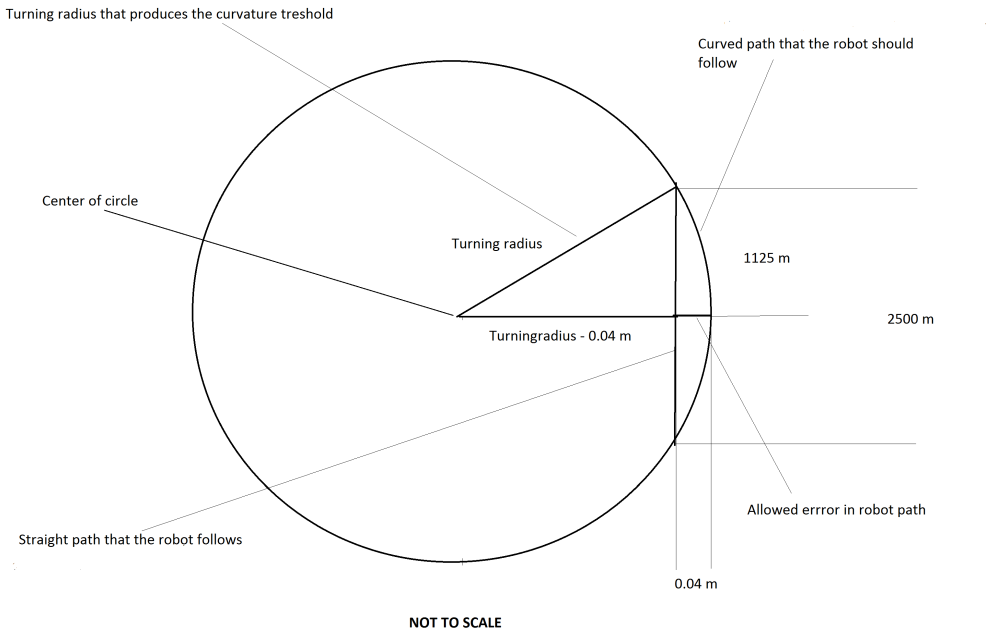

Figure 7.5: This figure shows how the singularity threshold can be found, given a constraint in precision of 4 cm.

As seen in figure 7.5 on the facing page we use Pythagoras:

$$\sqrt{R_t^2 - (|R_t| - 0.04)^2} = 1125m \tag{7.29}$$

And find the turning radius that produces the singularity threshold in curvature for the needed accuracy. A numerical value that satisfy equation 7.29 is $R_t = 1.58 \times 10^7 m$. This gives absolute curvature singularity threshold of $|\infty_t| = 6.3 \times 10^-8$, and whenever equation 7.11 outputs:

$$0 \leq |\infty_t| \leq 6.3 \times 10^-8 \tag{7.30}$$

A singularity is detected, and the path is assumed to be straight.

7.6.2 Propulsion Motor Kinematics

The propulsion motors that actuates the wheel speed has a gearbox connected to it with a reduction ratio of 60:1. The motors has maximum speed of 4400 RPM, this translates trough the gear box to maximum speed on the wheel of:

$$\frac{4400RPM}{60} = 73.3RPM \tag{7.31}$$

Since our wheel is 40 cm in diameter the maximum possible ground speed of the robot is:

$$\frac{73.3RPM}{60\frac{s}{min}} \times 0.4m \times \pi = 1.53m/s \tag{7.32}$$

Or around 5.5 kph, and this 100%. During a turn the outer wheel can maintain this speed, but the inner wheel has operate on a percentage of the outer wheel, as shown in equation 7.27 or 7.28 depending on whether the left or right wheel is the inner wheel. In essence, this mean that the robot can't move at full speed in turns, but it is unlikely that we will operate the robot under full speed, and thus can the outer motor be speeded up, whilst the inner motor speeds down, in order to hold constant velocity. The equation from ground speed S to RPM is:

$$RPM = \frac{60\frac{s}{min} \times 60}{0.4m \times \pi} \times S \tag{7.33}$$

And we can then include equation 7.33 into equation 7.28 and 7.27, and we get:

RPM Left Side Propulsion Motor

$$RPM_{ls} = \frac{60\frac{s}{min} \times 60}{0.4m \times \pi}\left(\frac{\sqrt{W_b^2 + (|R_t| - \frac{R_t}{|R_t|} \times T_w)^2}}{\sqrt{W_b^2 + |R_t|^2}}\right) \times S \tag{7.34}$$

RPM Right Side Propulsion Motor

$$RPM_{rs} = \frac{60\frac{s}{min} \times 60}{0.4m \times \pi}\left(\frac{\sqrt{W_b^2 + (|R_t| + \frac{R_t}{|R_t|} \times T_w)^2}}{\sqrt{W_b^2 + |R_t|^2}}\right) \times S \tag{7.35}$$

And we can calculate rpm commands that Roboteq motor controller can process and execute.

7.6.3 Servo Motors Positions

The steering servo motors that actuates the steering angles of the wheels also has a gearbox mounted to it, with the same reduction ratio as the propulsion motors. 60 motors turns counted by the encoder translates into 360°, since our robot steering range is from 15° to 345°, see section 7.5 on page 71, the number of turns that the motor can travel from left to right or opposite is:

$$60turns \times \frac{330^\circ}{360^\circ} = 55turns \tag{7.36}$$

We further assign 15 ° as zero turn and 345 ° as full 55 turns. Moreover we assumed that the motor has performed a home mode search successfully and therefore knows how man turns it has travelled. With this information available, we can modify the equations in section 7.5 on page 71 so the desired steering radius translates into unique number of turns N_t that the servo motor need to travel to. First the equation from degrees to number of turns is found:

$$Nt = \frac{\theta - 15^\circ}{330^\circ} \times 55turns \tag{7.37}$$

If we then include equation 7.37 into equations 7.23 - 7.26 we get:

Number of Turns Left Rear Servomotor

$$Nt_{lr} = \frac{180^\circ - \frac{R_t}{|R_t|} \times \arccos\left(\frac{|R_t| - \frac{R_t}{|R_t|} \times T_w}{\sqrt{W_b^2 + (|R_t| - \frac{R_t}{|R_t|} \times T_w)^2}}\right) - 15^\circ}{330^\circ} \times 55turns \tag{7.38}$$

Number of Turns Left Front Servomotor

$$Nt_{lf} = \frac{180^\circ + \frac{R_t}{|R_t|} \times \arccos\left(\frac{|R_t| - \frac{R_t}{|R_t|} \times T_w}{\sqrt{W_b^2 + (|R_t| - \frac{R_t}{|R_t|} \times T_w)^2}}\right) - 15^\circ}{330^\circ} \times 55 turns \quad (7.39)$$

Number of Turns Right Front Servomotor

$$Nt_{rf} = \frac{180^\circ + \frac{R_t}{|R_t|} \times \arccos\left(\frac{|R_t| + \frac{R_t}{|R_t|} \times T_w}{\sqrt{W_b^2 + (|R_t| + \frac{R_t}{|R_t|} \times T_w)^2}}\right) - 15^\circ}{330^\circ} \times 55 turns \quad (7.40)$$

Number of Turns Right Rear Servomotor

$$Nt_{rr} = \frac{180^\circ - \frac{R_t}{|R_t|} \times \arccos\left(\frac{|R_t| + \frac{R_t}{|R_t|} \times T_w}{\sqrt{W_b^2 + (|R_t| + \frac{R_t}{|R_t|} \times T_w)^2}}\right) - 15^\circ}{330^\circ} \times 55 turns \quad (7.41)$$

And we can calculate commands that servo motor controller can process and execute.

7.6.4 Example

Let us for simplicity use the equation $y = x^3$, in meters, as the path that the robot should follow. The center of the robot is assumed to move in a of speed S of 1 m/s and let us assume we use GPS information to know the x-value in meters along the path, then the turning radius is explicitly known for the whole path. We start by setting up equation 7.10 and 7.11 with our simple path's single and double derivatives included:

$$R_t = \frac{(1 + 9x^4)^{\frac{3}{2}}}{6x} \quad (7.42)$$

$$\infty_t = \frac{6x}{(1 + 9x^4)^{\frac{3}{2}}} \quad (7.43)$$

Let us further examine turning radius for the path $y = x^3$ for X-values given below:

X equal to -1

$$\infty_t(-1) = \frac{6(-1)}{(1+9(-1)^4)^{\frac{3}{2}}} \neq 0 \tag{7.44}$$

The singularity test, see section 7.4.1 on page 71, shows no singularity, and the turning radius is given by:

$$R_t(-1) = \frac{(1+9(-1)^4)^{\frac{3}{2}}}{6(-1)} \approx -5,3m \tag{7.45}$$

And this is expected, as this is a right turn section 7.4 on page 69 for the robot. The commands sent to the local end-effectors of the robot are[1]:

Left Front Wheel		Right Front Wheel	
Nt_{lf}	26.6 turns	Nt_{rf}	26.3 turns
RPM_{ls}	3323 RPM	RPM_{rs}	2413 RPM
Left Rear Wheel		**Right Rear Wheel**	
Nt_{lr}	28.4 turns	Nt_{rr}	28.7 turns
RPM_{ls}	3323 RPM	RPM_{rs}	2413 RPM

X equal to 0

$$\infty_t(0) = \frac{6(0)}{(1+9(0)^4)^{\frac{3}{2}}} = 0 \tag{7.46}$$

Singularity test reveals a singularity, and the message sent to the robot is that each of the four wheel should be 180° and have the same speed. And consequently the commands sent sent to the robots local end-effectors are:

[1]The presentation of commands sent to the robot for this example are placed "inside" a line drawing of the NMBU mobile robot, to make it more intuitive

Left Front Wheel		Right Front Wheel	
Nt_{lf}	27.5 turns	Nt_{rf}	27.5 turns
RPM_{ls}	2865 RPM	RPM_{rs}	2865 RPM
Left Rear Wheel		**Right Rear Wheel**	
Nt_{lr}	27.5 turns	Nt_{rr}	27.5 turns
RPM_{ls}	2865 RPM	RPM_{rs}	2865 RPM

X equal to 1

$$\infty_t(1) = \frac{6(1)}{(1+9(1)^4)^{\frac{3}{2}}} \neq 0 \tag{7.47}$$

Singularity test detects no singularity, and the turning radius is given by:

$$R_t(1) = \frac{(1+9(1)^4)^{\frac{3}{2}}}{6(1)} \approx 5,3m \tag{7.48}$$

And this also expected, as this place of the path is a left turn, and the commands passed to the robot are:

Left Front Wheel		Right Front Wheel	
Nt_{lf}	28.7 turns	Nt_{rf}	28.4 turns
RPM_{ls}	2413 RPM	RPM_{rs}	3323 RPM
Left Rear Wheel		**Right Rear Wheel**	
Nt_{lr}	26.3 turns	Nt_{rr}	26.6 turns
RPM_{ls}	2413 RPM	RPM_{rs}	3323 RPM

7.7 Advantages

It's worth noting that when singularity test senses a singularity, no more calculation is needed, and the straight path commands are sent directly to the motor controllers. It is advantageous that this calculation is the least complex, as this condition often will occur on the NMBU robots path.

When driving this robot from a joystick, the steering input to kinematics equations will probably be the curvature, instead of the turning radius. So that when the joystick steering knob is in home position, the curvature command is zero, and when joystick propulsion knob is manipulated, the robot while move in a straight line. If the steering knob is moved to the left, the curvature goes to positive number, where it's magnitude depends on the actual position of the joystick knob, and if the steering knob is moved to the right the same thing will happen, and only the sign of the curvature is changed.

Chapter 8

Minimizing wheel slip in uneven terrain

8.1 Measure Vertical Acceleration Proposal

Terrain capabilities can also be improved drastically when actuating each motor separately. Imagine the robots driving in a straight line on a flat surface , and were one of the wheels suddenly faces local heightening in the field. Whereas the remaining three wheels continues to run on the flat surface.

Notice that the distances the wheels will have to travel is different, see figure 8.1 on the next page, and since the robot is assumed to drive in a straight line, both the left wheels and the right wheels has the same angular velocity. With the conditions described above, this will force either the wheel facing the heightening to skid along because it should have been moving faster, or it will force the three remaining wheels to slip, because they should have been moving slower. A third outcome is also possible, and that is a change in the robots orientation, due to the skid-steer effect that occurs.

This mathematical imperfection gives us poorer terrain capability, more soil damage, and wastes fuel. The problem is not valid if a differential is used, like the one normal cars and tractors use, if they are driven under normal conditions. If they need to lock the differentials when climbing or driving in difficult terrain, the mathematical imperfections becomes valid here as well.

So the best solution would be to make the robot understand if one wheel faces a longer path, than the other wheel on the same wheelbase. And compensate for this by slowing down or speeding up the appropriate wheels independently, to avoid wheel slippage and the associated downsides. Since our robot can actuate each wheel independently, it is possible for our robot

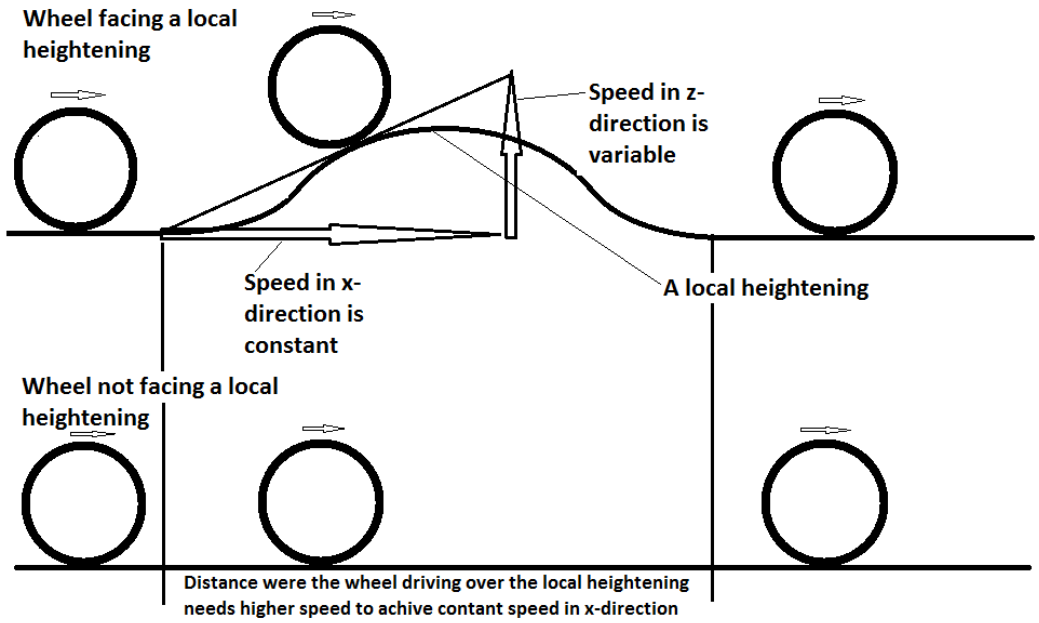

Figure 8.1: This figure shows the two different paths that wheels need to follow, and it is shown that the upper wheel in this figure needs to go faster during the event of the local heightening if the two wheels should be at the same x-coordinate at the same time.

to operate like that, and the challenge is to find a reasonable way to measure this difference in wheels speed. A solution might be to implement inertial measurement units IMU's in the wheels, that will sense if there are any accelerating in z-axis and then calculate the needed speed increase in each wheel.

The needed speed increase v_h for the wheel meeting the heightening is is proportional to the super positioned speed, see figure 8.1, divided by the speed in the x-direction as shown below:

$$v_h = \frac{\sqrt{(v_z)^2 + (v_x)^2}}{v_x} \tag{8.1}$$

The speed in the x-direction is known, and the speed in the z-direction can be found by integrating the z-acceleration given by the IMU in small time steps repeatedly:

$$v_z(t_{i+1}) = v_z(t_i) + \int_{t_i}^{t_{i+1}} \dot{v}_z(t_{i+1})dt \tag{8.2}$$

then the robot can move over bumpy terrain with minimal wheel slippages,

and maximum pull-force. This system obviously need to run in real time, but the robot is not moving fast at all, only 5 kph, and there should be time enough to carry out the computation. There is one immediate problem with equation 8.2, as the robot should respond equally by speeding up the wheel if there where a local heightening or hole in the ground, as both situations gives the wheel a longer path to travel, but it should slow down the wheel when it is starting reach the top of the local heightening. The direction of the acceleration is different, so some sort of mathematical tool, out side the scope of this thesis, is needed to account for this.

8.2 Constant Torque Proposal

Other ways of solving this problem is by making sure that each wheel faces the same torque, and make sure that it is not the lowest torque that is the reference. The reason for this can best be described by a situation encountered by many owners of cars with differentials; Suppose one wheel is on ice, and the other wheel is on tarmac, the if the vehicle is situated in just a tiny hill it won't move, and the reason for this is that the differential apply the same torque to wheel on the tarmac, as it generates from the wheel on the ice.

Since the wheel facing the local heightening is experiencing a "skid along" the torque is measured to be smaller than the rest of the wheels, and the the robot would have speeded up that particular wheel in order to maintain constant torque. A down side to this solution is that the torque varies with the friction against the surface, and if the heightening was slippery e.g icy, the wheel would just increase the RPM until it reach the upper RPM limit that has to be implemented to avoid unhealthy conditions for the motors, and possibly damage the surface.

8.3 Relevance for Mobile Agricultural Robots

The practical difference in the two proposals presented above might be small, and the easiest method to research more on is the torque model, as this type of sensing can be done in already bought equipment.

This system will be of great potential if the terrain is is bumpy. It also demands that the robot has a lot of flexibility in the suspension for it to be useful, and since the current version of our mobile agricultural robot is quite inflexible and the terrain it faces are mostly flat, this will probably not be implemented in this version of the robot.

Chapter 9

Conclusion

9.1 Part II

The conclusion regarding the main purpose of this work is that the kinematic equations for NMBU Mobile Agricultural Robot is found trough a geometrical approach used for graphical intuition.

Mapping from geometrical representation to vector representation is trivial. Inverse kinematics approach has unambiguous solution. Dynamics can be neglected since the operating speed is low and the gain in the closed loop motor controller is high. Crab steering has a trivial kinematic solution. Four wheel Ackerman steering is the main steering mode on NMBU Mobile Agricultural Robot.

Singularity conditions in the turning radius equation are avoided using a singularity test prior the turning radius calculation. Unique equations for all actuated joints are found. The input in these equation are either the velocity vector $[\dot{x}, \dot{y}, \dot{\theta}]^T$ or a turning radius and the velocity at the center of the robot, and the output is commands that the motor controllers can interpret, i.e RPM for the propulsion motors and number of turns for the servo motors.

Two proposals regarding traction in uneven terrain is contributed, both can improve accuracy and traction at the expense of complexity. At this stage of the project they are not needed, as the robot operates on a nearly locally flat terrain.

9.2 Introduction and Concept

Mobile Agricultural Robots should be light weight, so we can reduce soil compaction to a tolerable level, and thereby significantly reduce the energy used

on arable land. Robots make it possible to reinvent farming by performing operations not possible today, that either was found too expensive or time consuming. Precision farming done by a light weight robot will increase yield by reducing soil compaction, and reduce herbicide and pesticide usage to a minimum by treating only the weed(s). Small robots make public acceptance and liability easier, as collisions with humans becomes less fatale. Farmers hourly wage will increase since the robots can work at night.

9.3 Part I

This section presents conclusions made by the participants in this project, and they are mainly drawn from the literature search made earlier in this project.

Independent four wheel steering offers crab steering, maximum tool area, lowest power consumption, highest manoeuvrability and lest surface damage. Separately actuated components are energy efficient, reduce mechanical complexity, and maximize tool space. Integrated servomotor is good steering actuator as it has the lowest electrical complexity, fewest parts, and takes up minimal space. Planetary gear is the chosen reduction gear for steering actuators because of their high efficiency and compactness. Absolute single turn encoder mounted on the steering shaft is a precise feedback device for absolute position, but a cheaper inductive sensor is implemented in the robot.

Diesel has today 40 times higher specific energy $\frac{KWh}{kg}$ than state of the art commercially available batteries. Rechargeable lithium-ion battery pack is the best energy source for the robot, as this gives the robot zero CO_2 emissions whilst operating, and cleaner air and food. $LiFePO_4$ is chosen as chemistry since it is environmentally friendly, offers superior thermal and chemical stability for relatively small expense in specific energy. A four button emergency stop system is with one main solenoid contactor on each battery is implemented for safe operation. Robot need to be able to change battery packs automatically for prolonged autonomous operation e.g at night. Maximum voltage in the procured 48 V battery was significantly higher than the integrated 48 V servomotors could handle, and a larger literature review prior the procurement would have led to a 36 V battery.

An integrated servomotor for propulsion would offer, as mentioned above, lowest electrical complexity, fewest part, and takes up minimal space. A cost effective solution, with separate motor and motor controller is implemented. As motor runs unsteady backwards in closed loop speed mode using hall sensor as feedback, incremental encoder is procured. Planetary gear is the

optimal reduction gear for propulsion actuators, as mentioned above because of their high efficiency and compactness. A toothed belt connects the motor placed up in the frame to the wheel hub mounted planetary gear with 1:1 ratio.

Tracks continuous surface offers better mobility in terrain that is soft, contains obstacles of a certain size that can get jammed between, and has deep cracks in the ground. Wheels offer energy efficient propulsion with low mechanical complexity in a cost effective design and makes field tests of different steering schemes possible. 40 cm high snow blower tire is elected for energy efficient traction on various surfaces.

A steel and alloy glued combination makes the frame light weight and robust. Tool modules should be centred in the frame, giving equal weight on each wheel, creating maximum traction capabilities in the robot. The suspension is passively built in the frame, and when payload is present, it should flex and follow the terrain.

Bibliography

Anaheimautomation. Servo motor guide, 2013. URL http://www.anaheimautomation.com/manuals/forms/servo-motor-guide.php#sthash.dX4iv1JE.dpbs.

Anaheimautomation. Encoder guide, 2014. URL http://www.anaheimautomation.com/manuals/forms/encoder-guide.php#sthash.rhHhZMLa.dpbs.

ATC Autonomous Tractor Corporation. *The future of farming*. Autonomous Tractor Corporation, 4302 13th Avenue South Fargo, North Dakota 58103, October 2013. URL http://www.autonomoustractor.com/.

Bent S. Bennedsen. Selvkørende robotter gødsker og sprøjter. Technical report, AgroTech, september 2009.

Peter Biber. Personal communication, robert bosch gmbh. E-mail asking for specs and picture of Bonirob, March 2014.

Jonathan Billinger. Caterpillar challenger mt765b. This work is licensed under the Creative Commons Attribution-Share Alike 2.0 Generic Licence, October 2008. URL http://www.geograph.org.uk/photo/1023986.

Finn Bjerknes. New and old filling machines. Personal conversation with Finn Bjerknes, July 2012.

Nils Bjugstad. Personal conversation, May 2014. Soil compaction.

Simon Blackmore. Robotic agriculture; designing systems for the farm of tomorrow, November 2012. URL https://www.innovateuk.org/c/document_library/get_file?groupId=2828839&folderId=7196297&title=3+Simon+Blackmore+Robotic_Agriculture.pdf.

Fredrik Blomberg. Omnidirectional mobile aricultural robot. Master's thesis, Norwegian University of Life Sciences, 2014.

Deemencoders. How do absolute encoders work?, 2014. URL http://www.deemencoders.com/Howitworks.html.

J. DeJong-Hughes, J. F. Moncrief, W. B. Voorhees, and J. B. Swan. Soil compaction: causes, effects and control. Technical report, Regents of the University of Minnesota, 2001.

Machine Design. Selecting dc brush and brushless motors, 2009. URL http://machinedesign.com/motorsdrives/selecting-dc-brush-and-brushless-motors.

David Dorhout. Prospero robot farmer. Copyright 2013 Dorhout R and D LLC. All rights reserved., 2013. URL http://www.dorhoutrd.com/prospero_robot_farmer.

Yae Edan, Eldert van Henten, and Bart van Tuijl. Clever robots for crops. Presentation 11, Ben Gurion University AND Wageningen University and Research Centre, June 2011. URL http://www.crops-robots.eu/dissemination/workshops/2011-06_MechEng/Agricultural_Robotics_WUR-BGU.pdf.

Energilink-TU. *Diesel, mer populær enn noen gang.* Teknisk Ukeblad Media AS, 2008. URL http://energilink.tu.no/no/diesel.aspx.

James C. Frisby and Donald L. Pfost. Soil compaction: The silent thief. Publication G1630, University of Missouri, Department of Agricultural Engineering, Columbia, MO 65211, USA, 1993.

Pål Johan From. Personal conversation. Mathematical guidance, 2014.

Pål Johan From, Jan Tommy Gravdal, and Kristin Ytterstad Pettersen. *Vehicle-Manipulator Systems.* Advances in Industrial Control. Springer, Industrial Control Centre Glasgow scotland, UK, first edition, 2014.

Suresh Golconda. Steering control for a skid steered autonomous ground vehicle at varying speed. Master's thesis, University of Louisiana, Lafayette, 2005.

Ole Green. *Konskilde Robotti.* Kongskilde Industries A/S, 2013. URL http://www.kongskilde.com/in/da/News/Year%202013/09-09-2013%20-%20New%20automated%20agricultural%20platform%20-%20Kongskilde%20Vibro%20Crop%20Robotti. Collabriation with University of Southern Denmark and Conpleks Innovation ApS.

Lars Grimstad. Omnidirectional mobile aricultural robot. Master's thesis, Norwegian University of Life Sciences, 2014.

C Holm. Articulated, wheeled off-the-road vehicles. *Journal of Terramechanics*, Volume 7(1):19–54, 1970. Pergamon Press.

Industri Elektronik JVL Datasheet. *The MAC motor AC-servo motor with Integrated driver MAC50, 95, 140 and 141.* JVL Industri Elektronik, Blokken 42 DK-3460 Birkerød Denmark, 2014.

Industri Elektronik JVL Manual. *Integrated Servo Motors User Manual.* JVL Industri Elektronik, Blokken 42 DK-3460 Birkerød Denmark, lb0047-30gb edition, April 2014.

Alonzo Kelly. A vector algebra formulation of kinematics of wheeled mobile robots. Technical Report CMU-RI-TR-10-33 - REV 1.0, The Robotics Institute Carnegie Mellon University, 5000 Forbes Avenue Pittsburgh, PA 15213, Sept 2010.

J.-C. Latombe. *Robot Motion Planning.* Kluwer, Boston, MA, 1991.

Barrie Lawson. *Rechargeable Lithium Batteries.* Woodbank Communications Ltd 2005, Woodbank Communications Ltd, South Crescent Road, Chester, CH4 7AU, United Kingdom, 2014. URL `http://www.mpoweruk.com/lithiumS.htm`.

Tore Lervik. Personal conversation with altitec founder tore lervik, April 2014. URL `http://altitec.no/a123-2-3ah-3-3v-lithium-lifepo4.html`.

Tommy Ertbølle Madsen and Hans Lavdal Jakobsen. Mobile robot for weeding. Master's thesis, Technical University of Denmark, 2001. URL `http://www.unibots.com/Papers/mobilerobot.pdf`.

Fredrik Meltzer. Omnidirectional mobile aricultural robot. Master's thesis, Norwegian University of Life Sciences, 2014.

Lieve Meskens, Mieke Vandermersch, and Erik Mathijs. Implication of the introduction of automatic milking on dairy farms. Report, Departement of Agricultural and Environmental Economics Katholieke Universiteit Leuven, Lieve Meskens, Willem de Croylaan 42, 3001 Leuven, Belgium, August 2001.

Bjørn Fredrik Nielsen. Personal conversation. Mathematical guidance, 2014.

Randi Helen Nodeland. Melkeroboter gir bønder økt trivsel, 2013. URL http://www.forskning.no/artikler/2013/august/365725.

B. H. Nolte and N. R. Fausey. Soil compaction and drainage. Bulletin AEX-301, Ohio State University AND United States Department of Agriculture, Columbus, OH 43210, USA, 2013.

Wiliam Norris. *Modern Steam Road Wagons*, chapter Steering, pages 63–67. Longmans, 1906.

Timo Oksanen. Guidance of autonomous tractor with four wheel steering. Webinar 11, Aalto University, Finland Dept of Automation and Systems Technology, Aalto University School of Engineering P.O.Box 14100 00076 Aalto FINLAND, September 2013. URL http://www.fieldrobot.com/ieeeras/Downloads/20130926-Oksanen-Presentation.pdf.

pfeiferindustries. Timing belt advantages and disadvantages, 2014. URL http://www.pfeiferindustries.com/timing-belt-advantages-disadvantages-i-15-l-en.html.

Roboteq. *Advanced Digital Motor Controllers User Manual*. Roboteq, Inc, 7898 E. Acoma Dr. Suite 103 Scottsdale AZ 85260 USA, v1.3 edition, September 2013. URL http://www.roboteq.com/index.php/docman/motor-controllers-documents-and-files/documentation/user-manual/7-nextgen-controllers-user-manual/file.

Paul E. Sandin. *Robot Mechanisms and Mechanical Devices Illustrated*. McGraw-Hill, Inc., New York, NY, USA, 1 edition, 2003. ISBN 007141200X.

SEW-EURODRIVE. Sew eurodrive presentation. March 2014.

Benjamin Shamah, Michael D. Wagner, Stewart Moorehead, James Teza, David Wettergreen, and William Whittaker. Steering and control of a passively articulated robot. Technical report, Carnegie Mellon University, 2001. The Robotics Institute.

Sick. Inductive proximity sensors, 2014. URL http://www.sick.com/group/en/home/products/product_portfolio/industrial_sensors/pages/inductive_proximity_sensors.aspx.

Roland Siegwart, Illah R Nourbakhsh, and Davide Scaramuzza. *Autonomous Mobile Robots*. Intelligent Robotics and Autonomous Agents. The MIT Press, second edition, 2011. Cambrigde, Massachusetts.

Bill A. Stout and Bernard Cheze, editors. *CIGR Handbook of Agricultural Engineering*, volume 3. American Society of Agricultural Engineers, 1999.

Marit Kristine Svenkerud. Omnidirectional mobile aricultural robot. Master's thesis, Norwegian University of Life Sciences, 2014.

Rubens A Tabile, Eduardo P Godoy, Robson R. D Pereira, Giovana T Tangerino, Arthur J. V Porto, and Ricardo Y Inamasu. Design and development of the architecture of an agricultural mobile robot. *Engenharia AgrÃcola*, 31:130 – 142, 02 2011. ISSN 0100-6916. URL http://www.scielo.br/scielo.php?script=sci_arttext&pid=S0100-69162011000100013&nrm=iso.

User forum Tesla. Technical battery discussion. Tesla entusiast forum, June 2011. URL http://www.teslamotors.com/no_NO/forum/forums/technical-battery-discussion.

George B Thomas, Maurice D Weir, and Joel R Hass. *Thomas' Calculus*, chapter 13, pages 728–734. Pearson Education, Inc, 12 edition, 2010. ISBN 0-321-64363-1. Metric Edition.

Toyata. Facts about articulated steering, 2014. URL http://www.toyota-forklifts.se/SiteCollectionDocuments/PDF%20files/Facts-about-articulated-steering.pdf.

Richard Wolkowski and Birl Lowery. Soil compaction: Causes, conserns, and cures. Publication A3367, University of Wisconsin, College of Agriculture and Life Sciences, Cooperative Extension Publishing, 432N. lake St., Rm.231, Madison, WI 53706, May 2008.

Norges miljø- og
biovitenskapelige
universitet

Postboks 5003
NO-1432 Ås
67 23 00 00
www.nmbu.no